Preparation and characterization of nanocellulose from wheat bran
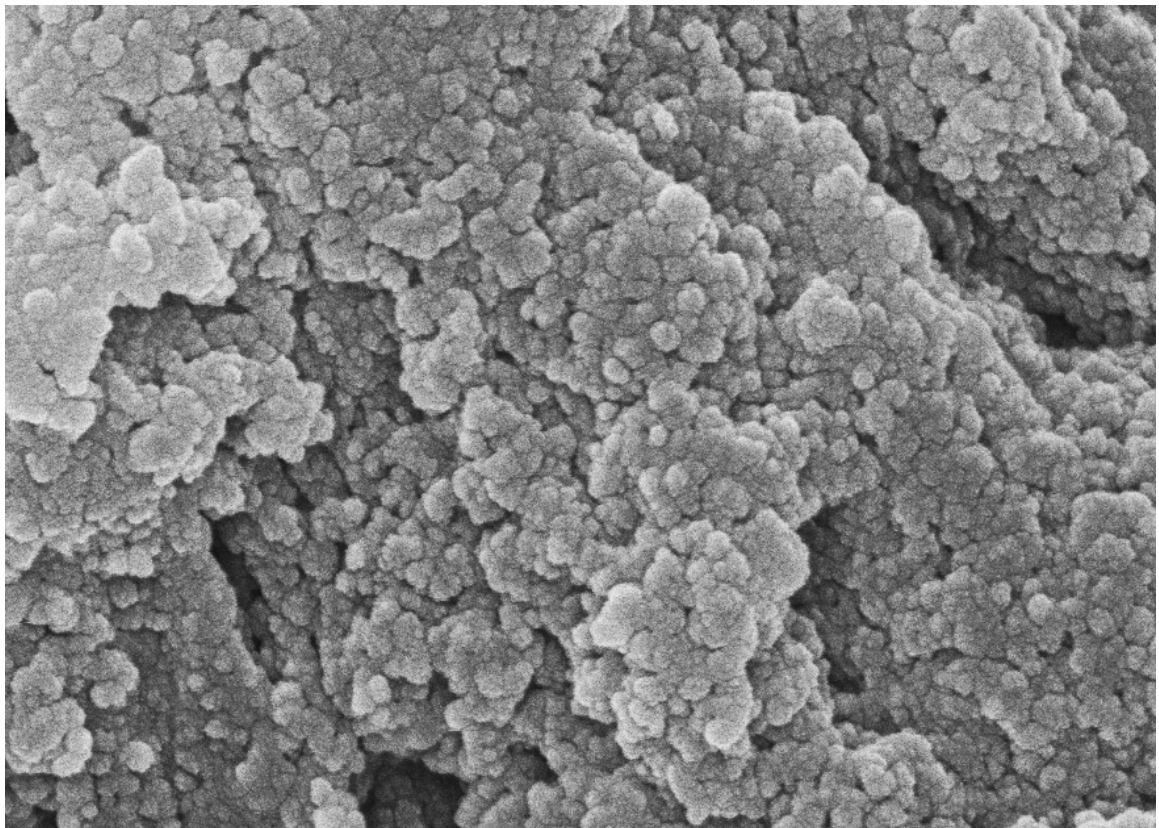

Claes Nilsson

LUND UNIVERSITY

Preparation and characterization of nanocellulose from wheat bran

by

Claes Nilsson

Department of Chemical Engineering
Lund University

April, 2017

Supervisor: **Senior Lecturer Mats Galbe**
Co-supervisor: **Professor Reine Wallenberg**
Examiner: **Professor Ann-Sofi Jönsson**

Preface

This report is the result of my master thesis that was carried out between October 2016 and April 2017 at the Kemicentrum in Lund. Most of the work has been done at the Department of Chemical Engineering and some at the Division of Material Science at the Department of Chemistry, Lund University. I would want to thank everyone at the chemical engineering department for all the support and taking the time to help me with all of the instruments.

First of all I would want to thank my supervisor Mats Galbe for all the comments and insights he has given me during the course of this thesis. And also that he has given me space to perform the experiments that I wanted, but still have been able to help me if I got stuck.

I also would like to give a thank you to my co-supervisor Reine Wallenberg for helping me get access to all the instruments and responsible persons at the Division of Material Science.

Special thanks to Laura Folkers for taking your time to help me with the powder x-ray machine and showing me all I needed to know about operating the machine.

In addition, Daniel Jacobsson deserves big thanks for helping me with sample preparations and giving me great tips of how to get good images of my samples with the scanning electron microscopy.

Thanks to Frank Lipnizki for giving me a nanocellulose sample and sending me good articles about the future of nanocellulose.

Thanks to Ann-Sofi Jönsson for giving me this opportunity to work with wheat bran and the production of nanocellulose.

Thanks to my officemates Miguel and Karl whom I shared a lot of laughter with and discussed many crazy topics.

Lastly I would like to thank my family for all the support and Camilla for having the patience to listen to me talking about nanocellulose and how great it is.

Abstract

Nanocellulose is being studied to a great extent around the world as it has great potential and many possible applications, for example, as an additive in greener polymers in a world where the need for replacements for fossil fuel based polymers increase. Different sources of cellulose are being considered for the production of nanocellulose as this can add value to what otherwise often is a by-product.

This study presents the feasibility of preparing nanocellulose from wheat bran cellulose and characterisation of the achieved material. The used cellulose had previously been extracted by an alkaline process, which removes most of the hemicellulose. The cellulose was converted to nanocellulose by acid hydrolysis and the suspensions were stabilised by ultra sound. The final products where characterised by Dynamic light scattering (DLS), Powder X-ray diffraction (PXRD) and scanning electronic microscopy (SEM). The extraction procedure yielded purified cellulose, i.e. crystalline spherical nanocellulose with a diameter around 100 nm.

Sammanfattning

Det forskas mycket runt om i världen på nanocellulosa, då nanocellulosa visar stor potential och kan ge stora fördelar till ett material när det adderas. Detta är också viktigt då arbetet att hitta grönare polymerer för att ersätta de som idag produceras från olja pågår för fullt för att minska miljöpåverkan. Detta har gjort att många studier har gjorts angående möjligheten att göra nanocellulosa från olika produkter som ofta anses vara en biprodukt i den berörda processen.

Denna studie tittar på möjligheten att göra nanocellulosa från cellulosa från vetekli och dess karakterisering. Cellulosan som användes hade tidigare blivit behandlad med alkali. Den konverterades senare till nanocellulosa genom sur hydrolys, därefter blev lösningarna stabiliserade genom ultraljuds behandling. Slutprodukterna blev analyserade med hjälp av dynamisk ljusspridring, pulverdiffraktion och svepelektronmikroskopi. Syrahydrolysen resulterade i renad cellulosa och analyserna visade att kristallina och sfäriska nanocellulosa partiklar hade bildats med en diameter på runt 100 nm.

Table of Contents

1 Background

1.1 Introduction

Wheat is grown all over the world and is only second by rice as the main human food crop, this means that wheat is a renewable and abundant resource. Wheat itself consists of different layers, the embryo (the germ), the endosperm, the aleurone layer, which encases the endosperm and the pericarp according to Figure 1.1. The fraction containing the pericarp and the aleurone layer is called bran.
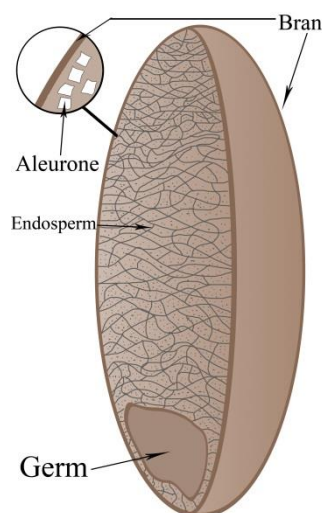

Figure 1.1. Schematic picture of wheat

Milling of wheat is one process of separating the endosperm from the embryo and bran layers. Endosperm is then milled to white flour while bran is a by-product [1]. Bran is to a large extent used as livestock feed, only a minor part is sold for food purposes, which is increasing as research has shown that bran with its high fibre content can give many health benefits [2].

Wheat bran is composed of cellulose, lignin and hemicellulose, the most abundant biopolymers on earth. While polymers today for the most part are made from petroleum, there is an interest of replacing petroleum-based polymers with renewable material made from biomass, providing they show similar properties and are price competitive [3]. Wheat bran accounts for up to 25% of the grain weight and is a by-product of the milling industry. If extraction of cellulose and hemicellulose becomes cost-efficient it can contribute to finding a sustainable replacement for petroleum-based polymers [2] [3].

The chemical structure of hemicelluloses can be modified to alter the properties and in this way be tailored for a specific purpose. Hemicellulose shows good film and oxygen-barrier properties, which makes hemicellulose-based polymers a candidate for different packaging applications [4]. The packaging sector accounts for a large part of the plastic products market, which makes incorporation of hemicellulose compounds very interesting [3].

Cellulose can also be extracted from wheat bran. It has a more crystalline structure in contrast to hemicellulose. When constituents like lignin, pectin and hemicellulose are removed from the wheat bran, highly crystalline cellulose remains and if the dimension of the cellulose

particles is in the nano-scale it can be called nanocellulose. Nanocellulose has many promising properties and applications, for example it is biocompatible, used as food additive, used in cosmetic products, paper strengthening, membrane material and is strong as Kevlar [5].

1.2   Aim and scope & Disposition

This report is a study of the possibility to convert cellulose from wheat bran to nanocellulose, where the wheat bran residue is from a solid fraction after hemicellulose has been extracted. Xylophane AB cellulose supplied the cellulose starting material. It was used for conversion of cellulose to nanocellulose and to evaluate the conversion of cellulose by microscope and x-ray diffraction. Cellulose was evaluated by different methods for determination of the possibility to make nanocellulose from wheat bran cellulose.

Chapter 2 gives a more detailed review of cellulose, nanocellulose, hemicellulose and other important aspects is presented.

In chapter 3 the different extraction and conversion methods are presented in more detail. The different characterisation methods of interest are discussed in chapter 4, Chapter 5 describes how the samples were prepared for the different methods. Chapter 6 details what instruments and to what specification it was used when analysing samples.

Chapter 7, 8 and 9 discuss the results, conclusions and a brief overview of future aspects.

2 Material of interest

2.1 Cellulose

Cellulose is present in many plants, which makes it almost an inexhaustible source of raw material; together with hemicellulose there is an estimated annual production in nature of 10^{11} -10^{12} t [6]. It was first chemically identified by Anselme Payen in 1838 and termed "Cellulose" from the French word *Cellule* "cell" in the French Academy 1839 [7]. Cellulose is a linear homopolymer consisting of D-glucose. Cellulose consists of glucose units that are 1 to 4 linked (β-1,4-glucosidic linkages, see Figure 2.1) making the repeating units in cellulose two glucose units (cellobiose).
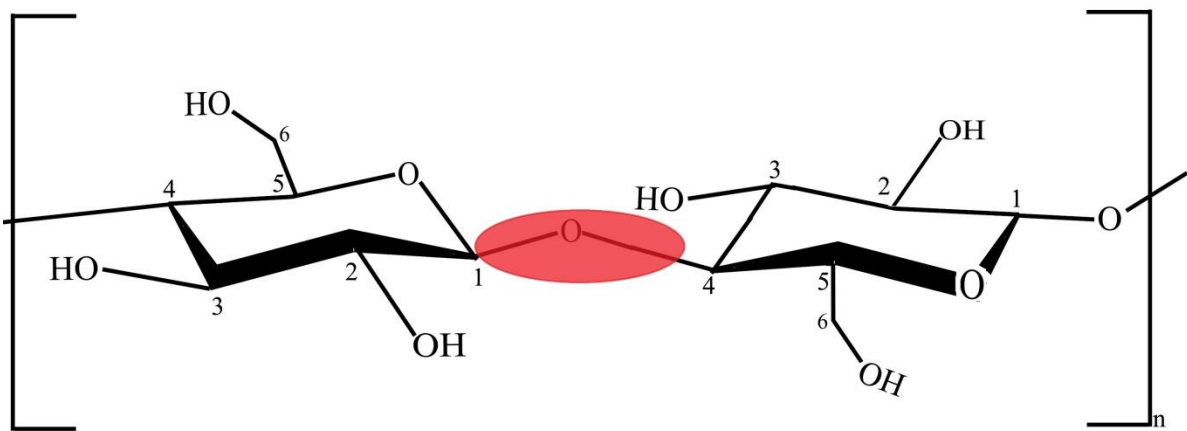

Figure 2.1 The basic repeating unit of cellulose, with the carbon number showing. The β-1,4 glycosidic bond, is the bond in red.

2.1.1 Applications

The function of celluloses in nature is to physically strengthen structures of plants. Cellulose together with lignin and hemicellulose help it stand upright and gives the branches its stiff exterior for example. Starch is also present in many plants and contains the same monomer as cellulose, i.e. glucose. They have, however, different physical and mechanical properties [8]. Starch consists of around 30 glucose units and is amorphous, nonlinear, soluble in water while cellulose is semi-crystalline and insoluble in water. Celluloses insolubility is often derived to inter-molecular hydrogen bonding which gives strong interactions between molecules. [9]

Cellulose is mainly obtained from wood pulp and cotton, where cotton is mainly cellulose and is widely used in the textile industry. Wood pulp, which contains cellulose and hemicellulose as well as lignin has been used for many decades to make paper. Interest has grown to use cellulose from wood pulp in the textile industry. If cellulose from pulp can be altered to present similar properties, cotton cellulose may be replaced to some degree, [10]. Cotton, which is high in cellulose content, has traditionally been used to make "guncotton". Guncotton is the cellulose ester of nitric acid, also called nitrocellulose. Nitrocellulose is a

white fibrous solid much like cotton or is a colourless liquid. Nitrocellulose is highly flammable and explosive when confined. Some major products that nitrocellulose is used for are smokeless gunpowder, inks, plastics, resins and lacquer coatings [11].

2.1.2 Structure

D-glucose is a relatively rigid molecule, which when polymerised gives cellulose its characteristic properties, hydrophilicity, easy degradability and chirality. Cellulose has a broad chemical variability because of the OH-groups reactivity. These groups also provide the basis for the extensive hydrogen bonding that gives cellulose a partially crystalline structure (Figure 2.2).
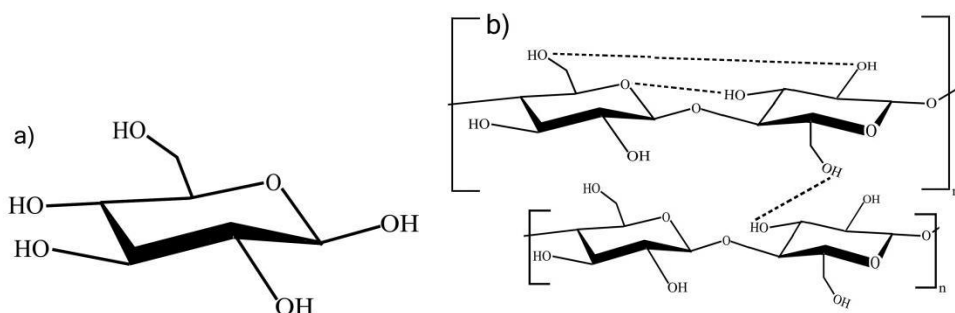

Figure 2.2. a) The molecule structure of D-glucose. b) A schematic picture of cellobiose. The dotted lines show OH-groups that contribute to the extensive hydrogen network and the OH-groups that give cellulose its chemical variability.

Solid state structure

Depending on the orientation of the hydroxyl groups in the structure, cellulose in its solid state can be found with areas of high crystallinity and amorphous regions. Different crystalline structures of cellulose exists: *cellulose I, II, III, IV* and *cellulose V. Cellulose I* and *II* are the most studied forms of cellulose. *Cellulose I* is present in two modifications I_α and I_β; the ratio of I_α/I_β varies depending on the source of the cellulose. The difference between I_α and I_β is their unit cell, which is triclinic for I_α and contains one glucose chain, while I_β has a monoclinic unit cell containing two parallel glucose chains (Figure 2.3). *Cellulose I* is thermodynamically unstable, but can be converted to *Cellulose II*, which has the most stable structure; therefore, it is the most desirable form of cellulose for commercial applications. [12]
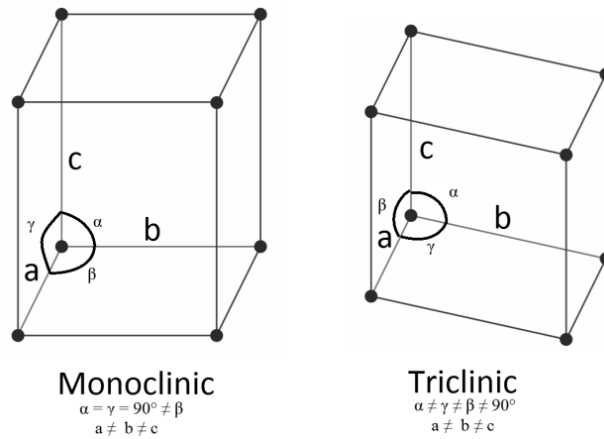
Figure 2.3. Overview of the monoclinic and triclinic unit cell

2.2   Hemicellulose

Hemicellulose is a name of a heterogeneous group of polysaccharides. This term is used differently, sometimes it is used for all polysaccharides except for pectin and cellulose. However, it has also been suggested that hemicellulose should be limited to groups of polysaccharides that has a well-defined structure like xyloglucan. Independent of definition hemicellulose is present in almost all land plants, usually in the primary walls. Hemicellulose binds with cellulose in the primary wall to strengthen it by using two types of interactions; one is entanglement with the cellulose micro fibril before crystallisation, and the other hydrogen bonding between OH-groups (Figure 2.4) [13].
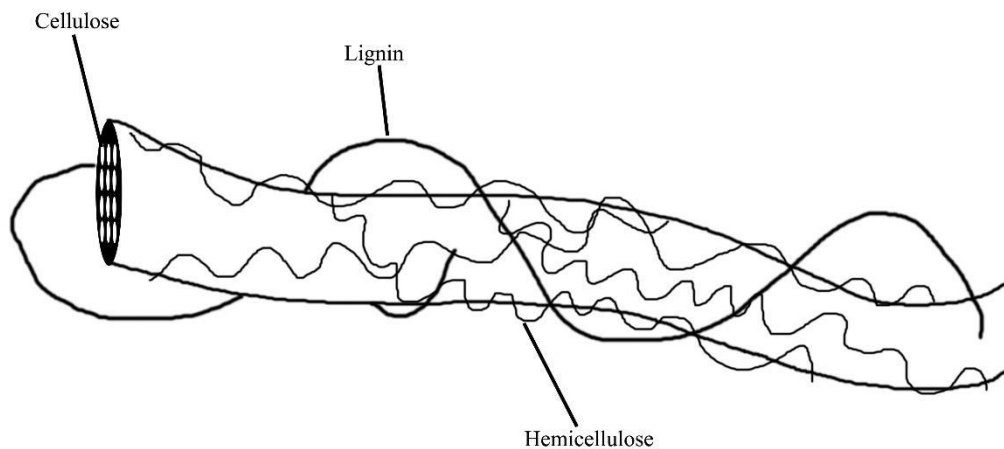
Figure 2.4 Schematic image over a plant wall where hemicellulose is entangled and has bonded to cellulose.

2.2.1 Applications

Depending on the polysaccharides that are used different applications can be considered. For example hemicellulose is used to make films for packaging because it is biodegradable and show good barrier properties, it is ideal for packing food and pharmaceuticals. It can be used in dyes, pigments and inks. It can also be used as a coagulant and a surfactant.

2.2.2 Structure

A single structure that perfectly describes hemicellulose does not exist, since it consists of a variety of different polysaccharides. Different polysaccharides can have common backbones, which makes it possible to organise them in different groups. Arabinose is a pentose, one isomer is shown in Figure 2.5,a. One source of arabinose is arabinoxylans, which also contain xylose. Xylose is a common hemicellulose and pentose and its structure is shown in Figure 2.5, b. [14]

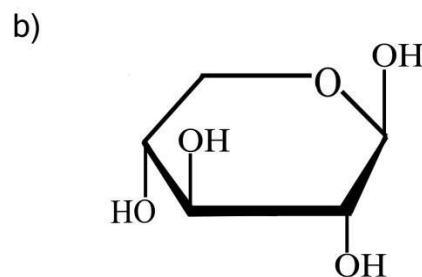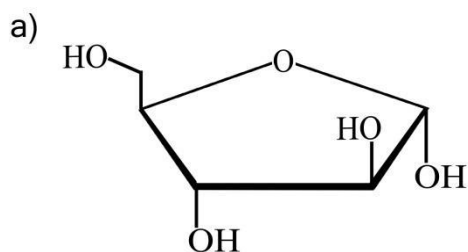Galactose is a glucose C4 (carbon number 4 can be seen in Figure 2.6 a) epimer where the OH is in an axial position instead of glucose's equatorial position. It can be viewed in Figure 2.6 [15]. Mannose is the C2 (carbon number 2 can be seen in Figure 2.6 b) epimer of glucose and is a monomer and is often found in mannan. An example of its structure can be viewed in Figure 2.6 [16]. Hemicelluloses are often highly branched, which prevents them from having a more ordered structure [13]. The crystalline part from a plant comes from cellulose, while both hemicellulose and lignin is amorphous [17].
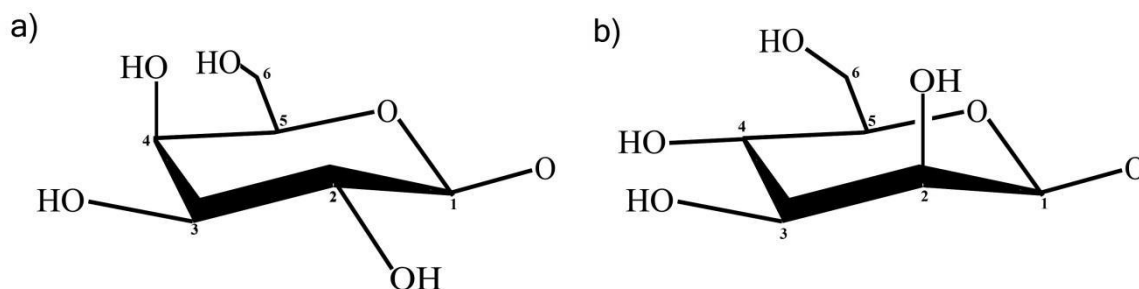

Figure 2.6. A shows D-galactoses molecular structure. B shows D-mannoses molecular structure

2.3   Lignin

Lignin is considered to be a thermoplastic polymer, the main monomer units are various ring-substituted phenyl propanes linked together. It is totally amorphous and hydrophobic, lignin is attributed for giving plants their rigidity [6].

2.3.1   Applications

Lignin has adhesive properties that can be enhanced by altering lignin itself. Therefore, it can be used in composite materials, rubber packing and as a co-monomer. It is used in building insulation made of glass wool, where lignin acts as a binder. It is added to human and pet food as a fibre source [18]. It can be modified to act as a thickener, flocculent for coatings and paints. Lignin has been suggested to be used as a slow-releasing coating for fertilizer and pesticide, for example a lignin gel that was used as a carrier for organic pesticide [18, 19].

2.3.2   Structure

Lignin is colourless or pale yellow but when treated with acid or alkali, the colour will shift into brown. Depending on the starting material, the resulting lignin will differ in chemical and mechanical properties because of the countless possibilities for the units in the structure to bond and orientate. The molecular mass of lignin is typically between 1000-20000 g/mol. The three basic repeating units of lignin are usually p-coumaryl alcohol, coniferyl alcohol and sinapyl alcohol (Figure 2.7). They account for the majority of repeating units in lignin, but other monomers can also be present. Naturally occurring lignin are to this day difficult to be studied, since when lignin is separated it is also altered. The intermolecular bonds are broken and surface chemistry is changed. [18, 20]
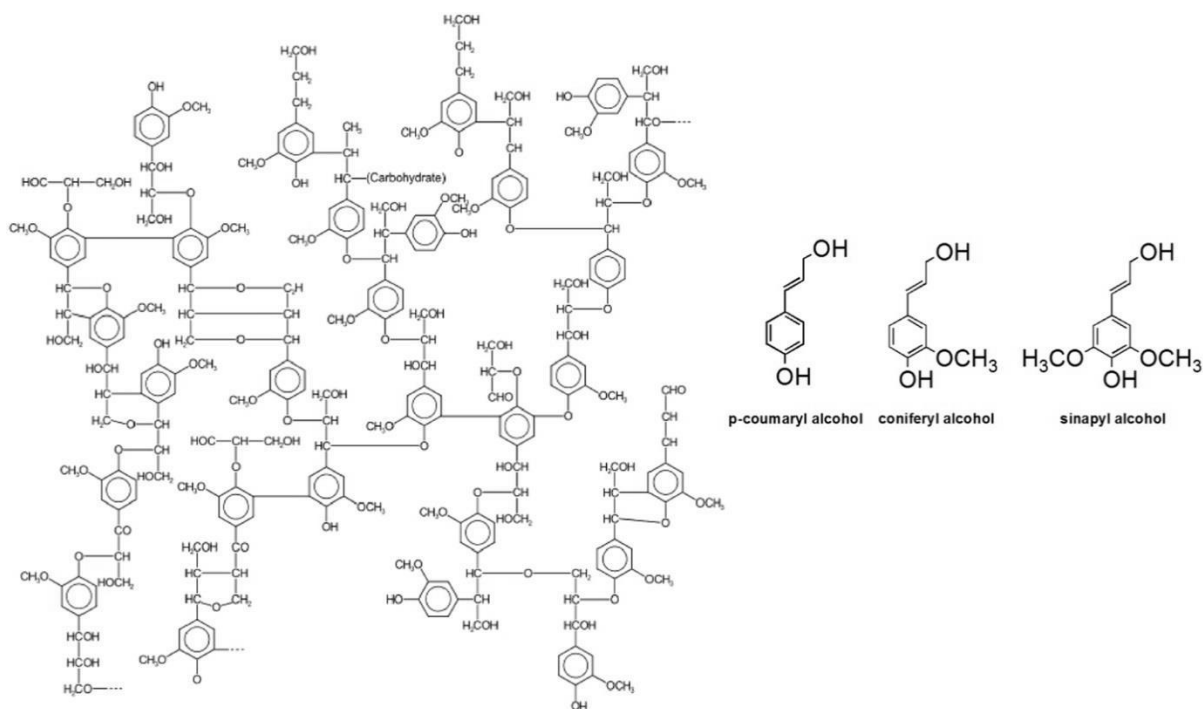
Figure 2.7. Example of typical lignin structure with basic repeating units

2.4   Nanocellulose

Nanocellulose (NC) is cellulose that has been processed to have nano-scale dimensions in width, length or both. NC is often divided into four different subcategories, *cellulose nanocrystals* (CNC), *cellulose nanofibrils* (CNF), *bacterial cellulose* (BC) and *spherical nanocellulose* (SNC). [21]

2.4.1   CNC

CNC is usually made using acid hydrolysis, where sulfuric acid is the most used acid. The hydrolysis aims to remove amorphous regions leaving highly crystalline particles that vary in size depending of cellulose source. From plant sources, the dimensions can for example be 5-20 nm x 100-500 nm. CNC has a rod-like structure with about 90% crystallinity. When sulfuric acid is used it grafts negatively charged sulphate half-ester groups (an dicarboxylic acid where only one of the acid groups have been esterified) onto the surface, which makes the particles repel each other through electrostatic repulsion; therefore, it prevents aggregation in aqueous suspensions. [21]

2.4.2   CNF

CNF is mainly prepared by mechanically destructuring cellulose. This can involve milling/grinding or high-pressure homogenization. Preparations can also be chemical treatment or enzymatic treatment, a combination of both chemical/enzymatic treatment with mechanical destructureing can occur. CNF does not have the same high crystallinity as CNC, but instead consist of both crystalline and more amorphous domains [5]. CNF is long entangled fibrils that can be micrometres long; therefore, width is usually the comparable

CNF dimension, depending on cellulose source and pretreatment, but vary from 10-100 nm [5], [21].

2.4.3 BC

Bacterial cellulose is a biopolymer formed by bacteria; the structure consists of fibrils and is less than 100 nm long; these fibrils are made up of much smaller nanofibrils that can be 2-5 nm. The high purity in the structure gives the material high water-holding capacity, high tensile strength and flexibility. BC is a bottom-up process, which means that no residue of lignin or hemicelluloses will be present in the material. This will for example reduce cost of purification. Other materials can be added to the culture medium to change the composition and properties of the final product. One negative aspect of this is that the final product cannot be altered, which can limit the possible applications. For example, BC-produced fibrils form a pellicle that has a water-holding capacity of 60-700 times its on dry weight [22, 23].

2.4.4 SNC

SNC made using acid hydrolysis, which is the same procedure as when making CNC. The material needs to be easily accessible during the hydrolysis to be able to make spherical particles. This can be achieved by swelling of the material; otherwise, spherical particles will be difficult to produce. The diameter is usually around 10-200 nm. Because of high tendency to form aggregates it has been suggested that these spheres is a product of self-assembled short rods. The spherical cellulose has been suggested to be able to replace CNC in different products, as it shows similar properties [24, 25, 26].

2.4.5 Applications

NC may form transparent films and has been proposed for many applications, for example food packaging because of good gas barrier, in electronics where ultrathin film exhibits piezoelectric response, which could be usable in flexible electronics. NC is used as a filler in thermoplastics to produce nanocomposites that are cost-efficient and have less negative impact on the environment. Because of NC properties it can be a stress-loading and load-bearing filler in thermoplastics. Usually the surface might need to be modified for it to be more compatible. NC shows good biocompatibility i.e. the possibility to be integrated for example into the human body, low toxicity, which makes it a good candidate for medical applications including drug delivery systems. [21]

3 Methods for preparation of nanocellulose

The cellulose used for conversion into nanocellulose, is derived from biomass. An overview of these conversions are presented in Figure 3.1. The conversion of biomass to cellulose will not be further discussed in this thesis, more information can be found in L.Brinchi, F. Cotana, E. Fortunati, J.M.Kenny "Production of nanocrystalline cellulose from lignocellulosic biomass: Technology and applications". [27]
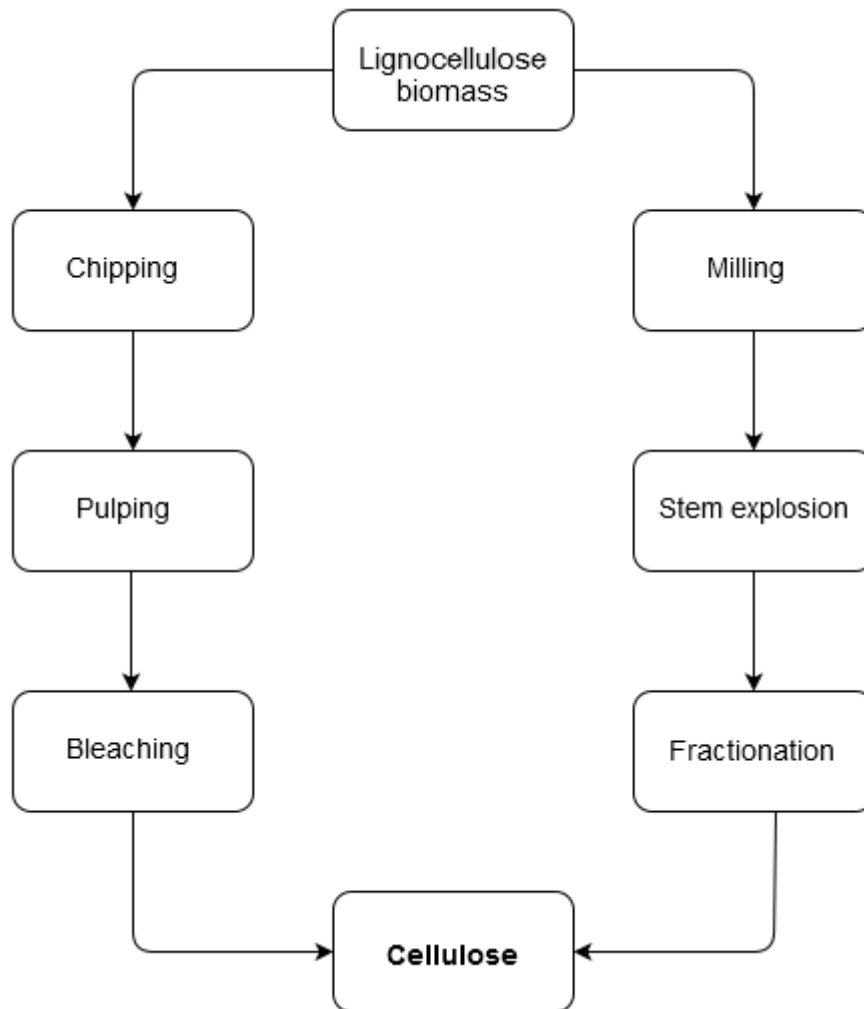
Figure 3.1. Overview of conversion methods of lignocellulose biomass to cellulose.

Three main conversion methods of cellulose to nanoparticles, acid hydrolysis, mechanical and enzymatic treatment, will be discussed in more detail below, followed by more unusual methods.

3.1 Acid hydrolysis

Acid hydrolysis is used for decreasing size of cellulose polymers. Studies show that acid affects both the amorphous and crystalline domains in cellulose; however, the amorphous part, being more branched and having a more open structure, makes it more accessible for the acid relative to the crystalline regions. The complete mechanism why amorphous regions are more affected by acid is not completely understood. [28]

The acid hydrolysis process is a result of the breaking of the β-1,4 glycosidic bonds in cellulose (see Figure 2.1) to depolymerise. The effects of acid hydrolysis are highly dependent on several variables. The result of the acid hydrolysis is affected by the source of cellulose that yields one type of nanocellulose, hydrolysis temperature, acid concentration, reaction time and what acid is used [29]. In literature the most commonly discussed acid is sulfuric acid being easily obtainable and relatively cheap [30, 31, 26]. It has been suggested that during hydrolysis a sulphate group can attach cellulose, which makes the surface negatively charged on the cellulose. This creates an electrostatic repulsion in the solution, which hinders aggregation. Ultrasonic treatment has been reported to be efficient for dispersing the nanoparticles. Negative environmental impact of sulfuric acid motivates a search for a replacement acid. One study (Xue Min Dong, 1998) found that optimal preparations for cellulose from cotton was; sulfuric acid (64%), pulp to acid ratio of 1:8.75, 1 h reaction time at 45 ℃ and a ultrasonic treatment for 5 minutes. Ultrasonic treatment can also be used for breakage of the polymer chains. If a sample is ultra-sonicated for a long time polymer chains will break to a large extent and the concentration of monomers will increase. The benefits achieved from ultrasonic treatment decreases after a sonication time over 5 minutes. [29], [32]

Microwave-emitting equipment can be used during the reaction to decrease the reaction time further; one study showed a reaction time of 10 minutes, when 60% sulfuric acid was used at 70 ℃, with reproducible results. [33]

3.2 Mechanical treatment

In general, mechanical treatment produces high shear forces on the cellulose structure that will break larger fibrils. Cellulose must be treated several times before nano-dimensions have been achieved. In addition, mechanical treatment is very energy consuming [28].

Typical mechanical treatment includes grinders and refiners where cellulose need to go through many cycles. To achieve better result for some material it can be beneficial to cool it before milling/grinding also known as cryocrushing. [28] Micro fluidisation is another technique where a liquid is pressurised and then pumped to a velocity of hundreds of meters per second; then the material is lead through a chamber which results in higher shear rates in the material and reduces particle size. [34]

3.3 Enzymatic treatment

Enzymatic hydrolysis is performed using enzymes, which are mixed together with cellulose. The enzymes will catalyse depolymerisation of cellulose. However, in enzymatic hydrolysis hemicellulose and lignin forms a physical barrier around cellulose. This will make cellulose inaccessible for enzymes and reduce efficiency. As enzymes sometimes bind irreversible to lignin this will reduce the overall efficiency. It means that more enzymes need to be added to achieve the same result as if added to lignin-free cellulose. Therefore, removal of hemicellulose and lignin prior to enzymatic hydrolysis is imperative for better conversion results [35, 36]. It is, however, possible to get cellulose nanofibrils from enzymatic treatment when other compounds have been removed leaving only cellulose [37]. Some studies show a more entangled network after enzymatic hydrolysis and the cellulose surface is also not negatively charged compared to acid hydrolysis, which could be desirable in some commercial end products. [38]

3.4 TEMPO Oxidation

2,2,6,6-tetramethyl-1-piperidinyloxy (TEMPO) is a water-soluble and a stable radical compound. It is used for highly selective oxidation of the C6 hydroxyl group (see Figure 2.1) to carboxyl in a pH range of 10-11 in water. A decrease in polymerisation degree results and nano-scale particles can be achieved with the use of mechanical treatment of oxidized cellulose. This method of preparation of nanocellulose shows that individual nanocellulose fibrils can be formed and isolated because of the oxidation. To form individual fibrils a certain density of carboxylate must be common in the cellulose. During TEMPO oxidation, nanocellulose with crystallinities of 65-95% can be obtained. [39], [40], [41]

4 Characterisation methods

The selected characterisation methods depend on the choice of the properties that are to be determined. The methods should be chosen to make it easy to compare between samples and also give reliable results. In this thesis, the selected properties of interest include the following:

Crystallisation degree and crystal structure
In the literature, the most common method to determine cellulose crystallinity is *x-ray diffraction* (XRD), however the samples need to be dried in advance, which will affect the results as the structure changes upon drying.

XRD patterns can be used to determine the crystal structure by looking at the peaks in an XRD pattern. A pattern is based upon constructive and destructive interference by the scattered waves from the crystal structure when hit by the XRD beam. Figure 4.1 shows a primitive unit cell, if repeated it will describe a whole structure. Cellulose unit cells vary as mentioned in 2.1.2, depending on what cellulose structure it is. C*ellulose I* for example, the unit cell can be either monoclinic or triclinic which can be seen in Figure 2.3. The planes in the unit cell, shown in Figure 4.1, are repeated throughout the structure. When hit by an XRD beam the scattered waves from these plane interact and create a constructive interference that propagate and will be detected and results in a peak corresponding to the one in Figure 4.2 for the plane *002* which is the highest peak in the figure. If there is a crystalline structure present in the cellulose sample then it will have planes consistent with its unit cell, similar to the planes corresponding to the primitive unit cell.
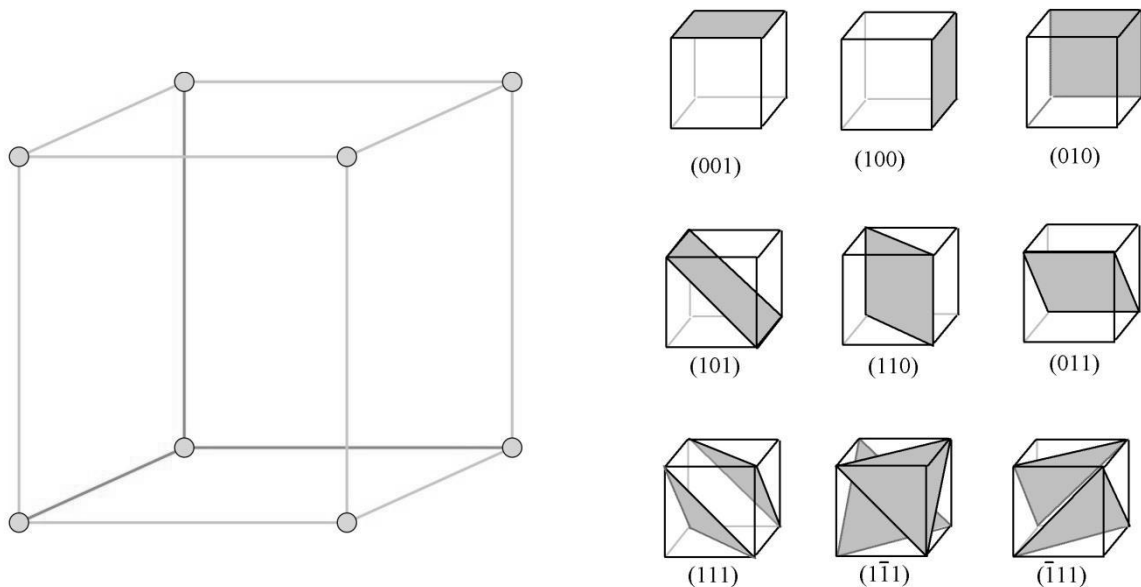

Figure 4.1. Primitive unit cell (left) and planes in the unit cell highlighted (right)
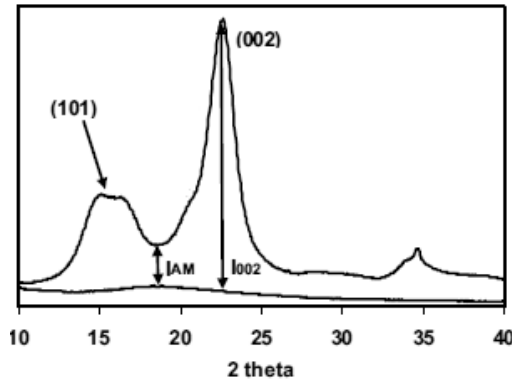
Figure 4.2.Overview of XRD pattern for crystalline cellulose I

For *cellulose I* there are different peaks corresponding to different planes, the 2θ angles for the planes *101*, *10ī*, *021*, *002* and *040* are the following; 14.7, 16.6, 20.6, 22.5 and 34.7. *Cellulose II* has the following planes; *101*, *10ī*, *002* and *040*. These have the following 2θ angles; 12.3, 20.1, 21.9 and 34.7 [42]. Crystallinity can be calculated from XRD patterns using different methods, where the most common is "peak height method", which is used for comparing the crystallinity between samples with the structure of *cellulose I* [43]. It uses the height of the I_{002} peak at 2θ angle around 22 degrees. Comparing this with the height of the minimum between the I_{101} peaks at 2θ angle between 14-16 degrees (see figure 4.1), can give an estimate of the crystallinity according to equation   (*1*. [43, 44].

$$C = 100 \cdot \frac{I_{200} - I_{am}}{I_{200}} \ (\%)$$ (1)

Where I_{200} is the *002* plane in *cellulose I* unit cell and I_{am} are the amorphous parts in the structure.

Particle dimensions/Particle size distribution
Electron microscopy can be utilized where a large amount of individual crystals are measured to statistically ensure measured particle size. Dynamic light scattering (*DLS*) can measure the particle size when it is in solution by using Brownian motion of the particles. Incapability of differentiating between aggregation of particles and single particles will affect the result. Size-exclusion chromatography (*SEC*) is used to determine polymer size and polydispersity by help of a calibration curve. By using different sizes of the pores in the column packing, particles will interact with the stationary phase depending on their size, which will yield varying retention times. Therefore, larger particles will elute first followed by smaller ones. If interactions between the polymer and the stationary phase happen the results will be affected. Interactions will lead to longer retention time; because the interactions and not only the size of the particles will affect retention time, and therefore lead to the conclusion that the particles are bigger or smaller depending on the interaction.

14

Morphology

Electron microscopy comprises of several methods, e.g. scanning electron microcopy (*SEM*) or transmission electron microcopy (*TEM*), scanning tunneling microscopy (*STM*), or atomic force microscopy (*AFM*). They can be used to determine the morphology of the converted cellulose. As samples studied in electron microscopy represent only a very tiny fraction of a material, this sample must be a good representative for the whole material to a high degree. This can be very hard if sample preparations include drying and dilution. To minimize analytical errors many samples must be studied to exclude unique morphologies present in one sample only.

5 Experimental

5.1 Materials

A cellulose/hemicellulose slurry was a gift from Xylophane AB. All sulphuric acid was supplied from AppliChem (72% w/w) and hydrogen chloride from Sigma-Aldrich. A sample of microfibrillated cellulose with the trademark Exilva was supplied by Borregaard A/S in Sarpsborg, Norway.

5.2 Methods

Acid hydrolysis was used for the conversion to nanocellulose. The work in this thesis was focused on conversion and characterisation of nanocellulose; therefore, yield is of less importance. It was decided to utilize well-documented acid hydrolysis instead of the less frequently investigated TEMPO oxidation, which shows higher yield for example. As cellulose from wheat bran is not studied to a great extent, the reaction parameters were adjusted for wheat bran.

5.2.1 Analysis of starting material

The extracted material from Xylophane AB has a pH of approximately 14 as a result of an alkali pretreatment to remove hemicellulose. To confirm if hemicellulose had been removed, 500 grams of wet, solid material was centrifuged and the supernatant was analysed according to the National renewable energy laboratory (NREL) procedure "Determination of Structural Carbohydrates and Lignin in Biomass" [45].

The slurry was diluted with deionized water and then filtered to neutralise the liquid. The filtered water was then analysed in the same manner as previously described [45]. The sediment was diluted with deionized water and 1 M HCl was used to adjust pH to approximately 8. After filtration of the solution, the sediment was washed with deionized water until a pH of 7.

To determine if pretreatment was needed prior to isolation of cellulose, a solid sample was prepared and analysed according to the NREL procedure "Determination of Structural Carbohydrates and Lignin in Biomass" [45] to analyse for monosaccharides and lignin.

5.2.2 Preparation of nanocellulose

All aqueous suspensions of nanocellulose were prepared in the following manner: washed and neutralised cellulose was hydrolysed with 72% (w/w) sulfuric acid using the setup shown in Figure 5.1

Pulp-to-acid ratio was kept constant at 1:20, the reaction times were between 1-5 hours at two different temperatures 45 and 50 ºC and stirring was applied. The reaction was stopped by adding a 10-fold excess of deionized water according to D. C. Arup Mandal and João Paulo Saraiva Moraisa [30, 31].

The suspension was cooled to room temperature. It was then centrifuged and the supernatant was removed while the solid was washed with deionized water and centrifuged again. This cleaning step was repeated several times until a pH around 7 was reached, leaving the suspension turbid, which indicates that small particles could be present. Some suspensions were then sonicated for five minutes to prevent aggregation of the particles. All suspensions were stored in a refrigerator at 7 °C.
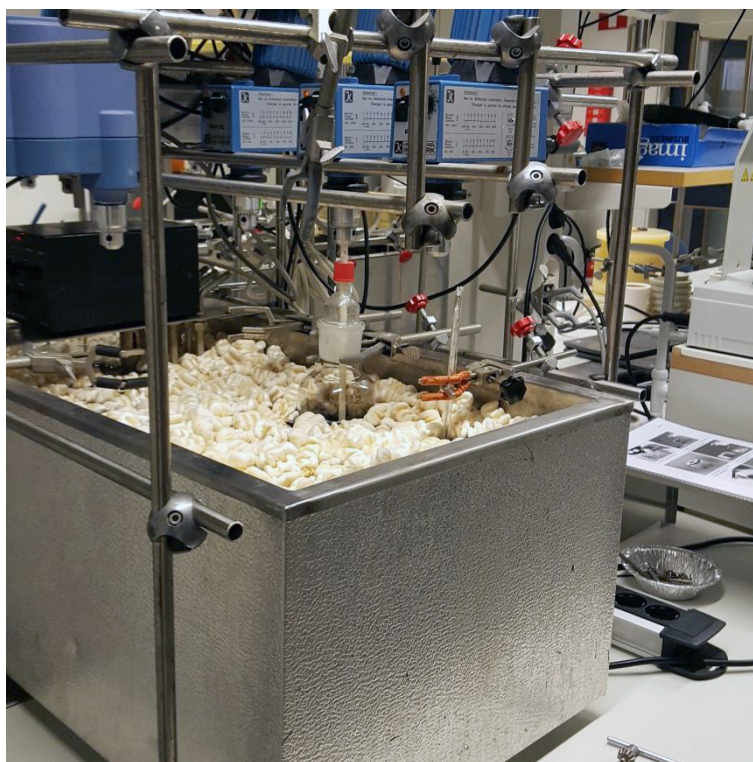

Figure 5.1.Overview of acid hydrolysis setup

5.2.3 Preparation of DLS samples

Around 1.5 ml solution was taken from every sample, which had been stored in the refrigerator, with a pipette. The solution was transferred to an Eppendorf tube and centrifuged to remove all the larger particles in solution. The supernatant were transferred to a new Eppendorf tube and then to a plastic cuvette. This plastic cuvette was then placed in the instrument for DLS analysis.

5.2.4 Preparation of SEM samples

2 ml solution was transferred to an Eppendorf tube and centrifuged. Then the supernatant was collected in a new Eppendorf tube. A sample holder for SEM can be seen in Figure 5.2. The samples were prepared using the following procedure: The surface of the sample holder was covered with non-conductive tape. The solution was distributed on this tape and the sample holder was placed in an oven at 70 °C. When the solvent had evaporated the sample holder was collected and placed inside a sputter instrument where an approximately 15 nm thick layer of Au/Pd was coated on the dried solution.

Figure 5.2. Sample holder for SEM, which can hold three individual samples. These can be inserted into the microscope at the same time. In this image the samples have been sputtered with Au/Pd layer.

5.2.5 Preparation of XRD samples

All samples for XRD were prepared by drying the solution in an oven at 45 °C for at least 48 hours. As nanocellulose was suspended in the liquid and had a tendency to aggregate, optimal sample preparations for XRD analysis were hard to achieve. The dried particles where grinded to get a uniform size and then placed upon a tape in a sample holder according to Figure 5.3, where a sample holder for XRD can be seen with a sample loaded. When the above method was not successful, another solution can be seen in Figure 5.4. Where a small amount of solution was placed in a pipette and the bottom of the pipette was covered with tape, while the top was cut off to promote evaporation in the oven. This allowed for the particle to dry directly upon the tape for XRD analysis, which also led to a more uniform distribution of particles over the tape. Parts of the sample aggregated to form a film when dried, which could be analysed in reflection mode instead of transmission assuming that the surface of the dried material represents the bulk of the material as well.
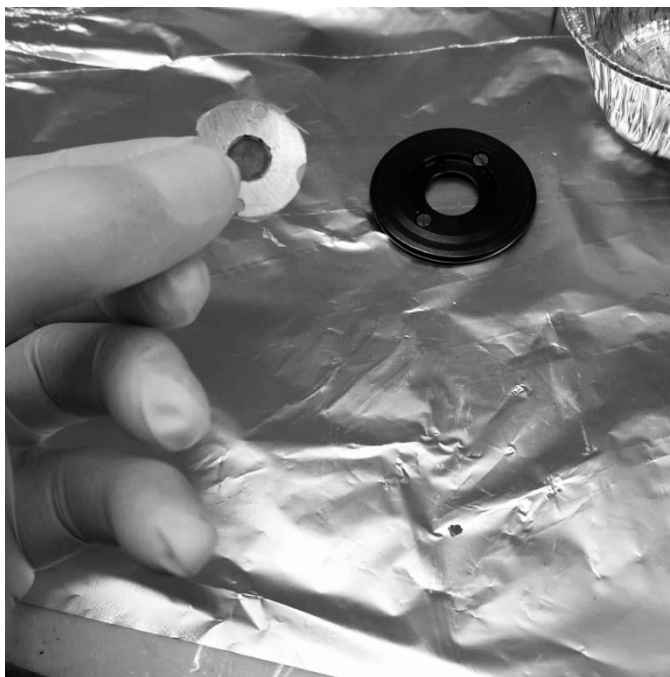
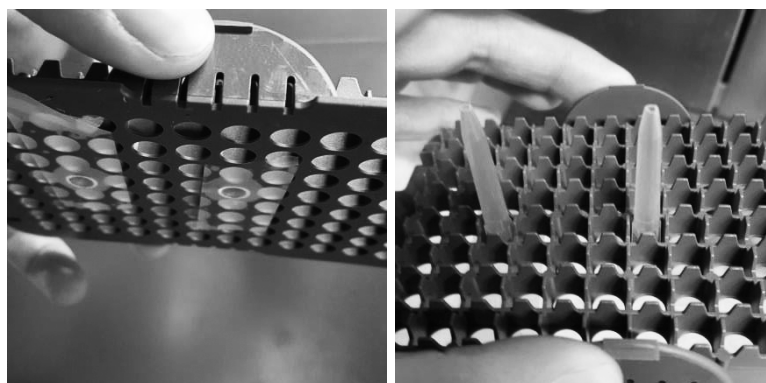*Figure 5.3. Sample holder for the XRD with loaded sample*

Figure 5.4. Pipette solution for drying the samples for XRD for better distribution of particles on the tape

6 Characterisation methods

6.1.1 Sugar analysis of NREL samples
Suger content was analysed using a Dionex Corp. (Sunnyvale, CA) ICS-3000 chromatography system with pulsed amperometric detection and a Carbo Pac PA1 analytical column. Deionized water was used as the eluent at a flow rate of 1 ml/min, and the column was washed with a solution of 200 mM NaOH in 170 mM sodium acetate. The sample injection volume was 10 µl, and D-glucose, D-galactose, D-mannose, D-xylose and L-arabinose from Fluka Chemi AG, Buchs, Switzerland was used as calibration standards.

6.1.2 X-ray diffraction (XRD)
Powder X-ray diffraction data were collected using a STOE StadiMP with Cu kα radiation at 40 kV and 40 mA, scattered radiation were detected in the range 2θ= 6-44° at 4.8°/minute for the cellulose samples.

6.1.3 Dynamic light scattering (DLS)
Measurements of particle size were made with a Malvern Zetasizer Nano – ZS instrument. Analyses were made under the conditions: Temperature 20 °C, particle refractive index 1.47, particle absorption coefficient 0.100 and water as solvent. Every sample was measured in three cycles where one cycle was ten times for ten seconds. Around 1.5 ml of sample was placed in a glass cuvettes and placed in the instrument.

6.1.4 Scanning electron microscopy (SEM)
The photographs of treated and untreated wheat bran cellulose were captured using a JOEL JSM-6700F field emission scanning electron microscope, with an acceleration voltage of 10 kV and a secondary electron (SE) detector was used to capture the images. Samples were coated with Au/Pd with an approximate thickness of 15 nm using a Balzers SCD 004 sputter coater instrument.

7 Results and discussion

7.1 Preparation of material

7.1.1 Raw material analysis

The remaing solids after extraction of hemicelluloses in wheat bran was used as raw material. The total dry solids (TDS) content of the slurry containing solids was 13 wt%. The analysis according to NREL "Determination of Structural Carbohydrates and Lignin in Biomass" [45] of liquid from the starting material before washing and neutralising showed that arabinose is present, together with other unidentified compounds. The initial concentration of arabinose present in the starting material before any hydrolysis have been done cannot be determined without identifying the other compounds and using an appropriate standard for calibration and calculations. The unidentified compounds are of less interest since they were solubilized. In this work, the solid material has been the main focus. After washing of the solid fraction most of the unidentified compounds will be removed. Results of the liquid concentrations of monosaccharides from a sample that had been neutralised with HCl acid and then washed with deionized water is shown in Table 7.1. Unidentified compounds were not present in this sample, which indicate that these compounds were polysaccharides that were converted to their monomeric form during acid hydrolysis.

Table 7.1. Concentrations of monosaccharides in filtered liquid

	Amount	Amount	Amount	Amount
	mg/L	mg/L	mg/L	mg/L
	Arabinose	Galactose	Glucose	Xylose
Sample 1:1	97	5.5	13	79
Sample 1:2	97	5.5	13	79
Sample 1:3	97	5.5	14	79

Table 7.1 shows that arabinose, xylose, galactose and glucose is present, which indicates that the filtered liquid mainly consists of different hemicelluloses, and glucose.

In Table 7.2 the concentration of glucose in the solid is considerably higher than in the filtered liquid shown in Table 7.1.

Table 7.2. Percent (w/w) of monosaccharides in solid material after washing and neutralisation

	Arabinose	Galactose	Glucose	Xylose	Mannose	Lignin
Sample 1:1	15.3	1.43	47.8	23.8	2.94	8.13
Sample 1:2	16.0	1.49	50.1	24.9	3.06	8.27
Sample 1:3	16.2	1.48	50.7	25.2	3.11	8.56

Lignin is also present in the solid. The amount was determined by a composition analysis of the starting slurry according to the calculations in the procedure used from NREL [45]. An

acid insoluble lignin of 8.21 ± 0.18 %, and an acid soluble lignin of 0.11 ± 0.004 % were found in the solid material. This gives a total lignin value of 8.32 ± 0.18 % in the starting slurry from Xylophane AB.

This indicates that most of the hemicellulose was removed from the solid material. The conversion of the cellulose to nanocellulose by acid hydrolysis will further increase the relative amount of glucose in the solid, as more of the hemicellulose will become dissolved in the acid according to Carvalheiro et al. [46]. An NREL analysis [45] was performed of the hydrolysed material. Glucose was the only detectable monosaccharide which indicates that the samples mainly consist of glucose. The lignin amount was reduced to 2.9 ± 0.7 % of the TDS content.

7.1.2   Conversion

The acid hydrolysis at both temperatures (45°C and 50°C) resulted in a pattern where a darker solution was obtained at longer reaction times. As the solution cooled to room temperature more and more particles aggregated, while solutions with longer reaction times stayed darker then the solutions with shorter reaction time, which is shown in Figure 7.1. The same pattern can be seen at both hydrolysis temperatures.

Figure 7.1. Acid hydrolysis time starts to the left with one hour and end with a reaction time of 5 hours to the left, with one hours increase between the cuvettes

This indicates that smaller particles were present in solutions with longer reaction times. As aggregation occurred smaller particles can have formed aggregates with larger particles; therefore, small particles may be present in solutions with shorter reaction time. After washing and centrifugation of the suspension, they were sonicated for five minutes to prevent particles from aggregating. This seemed to work as the sediment on the bottom was less compared to samples that had not been sonicated.

7.2   DLS analysis

7.2.1   45 °C

The first set of DLS analysis was performed on all solutions after acid hydrolysis at 45 °C. They were not sonicated after the washing and centrifugation procedure. An overview of the results can be found in Table 7.3

Table 7.3. Mean diameter of particles from acid hydrolysis at 45 °C with standard deviation.

Reaction time (h)	Mean particle diameter (nm)	Std.dev (nm)
Before acid hydrolysis	inconclusive	-
1	1631	44.5
2	1001	20.9
3	642	11.8
4	1111	46.5
5	1113	27.8

DLS analysis of the solution before acid hydrolysis gave inconclusive results, as particles had a too wide size distribution, which resulted in inconclusive or unmeasurable samples. Figure 7.2 displays a sample before acid hydrolysis, where particles of millimetre size can be seen.
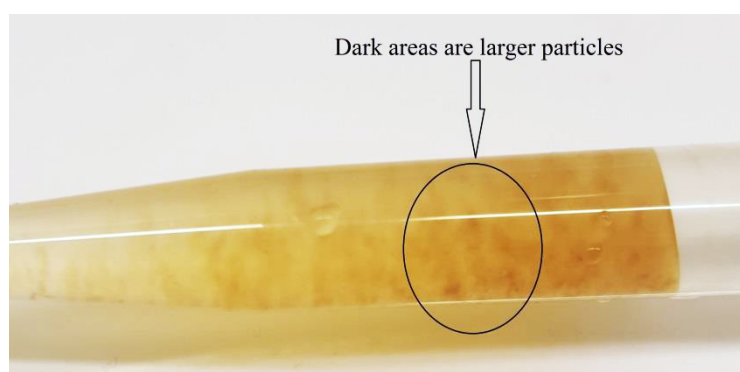

Figure 7.2. Picture of untreated material dissolved in water where big micrometre particles can be seen.

The results from DLS analysis indicate that acid-treated solutions show no correlation between reaction time and diameter. Only solutions with a reaction time of three hours deviate with a smaller diameter then the rest of solutions. From the literature [28], it can be concluded that there can be a correlation between diameter and reaction time. During acid hydrolysis, the β-1,4 glycosidic bond is broken, which in return will shorten the polymer chains and thus decreasing the physical dimensions. This would suggest that longer reaction time will lead to a smaller particle diameter; however, this relationship is not seen in Table 7.3. This indicates that either the acid hydrolysis was unsuccessful, or the particle aggregation occurred to a greater extent than assumed.

7.2.2 50 °C

These suspensions were washed and centrifuged using the same procedure as for the solutions at 45 °C; in addition, they were also sonicated to prevent particle aggregation in solution. The results presented in Table 7.4 show no correlation between reaction time and particle diameter, which is similar to the results achieved after acid hydrolysis at 45 °C. The mean particle diameter, however, is much smaller in solutions after hydrolysis at 50 °C. Even if the temperature would increase the hydrolysis rates of β-1,4 glycosidic bonds it is more likely that sonication of the solution prevented aggregation of particles to the same extent. This is a likely explanation since the temperature difference is five degrees only, and the two different hydrolysis temperatures give basically the same results.

Table 7.4. Overview of the samples mean diameter with standard deviation from acid hydrolysis at 50 °C

Reaction time (h)	Mean particle diameter (nm)	Std.dev (nm)
Before acid hydrolysis	inconclusive	-
1	224	5.7
2	316	5.9
3	226	1.4
4	360	2.6
5	359	1.7

Table 7.3 and Table 7.4 data suggest that aggregation may occur in solution to a great extent, but that it is counteracted by sonication. Acid hydrolysis was successful as nano dimensions of particles were achieved, which can be seen in Table 7.4. However, as aggregation of particles will lead to an overestimation of particle diameter using DLS, further analysis will be needed to determine a more precise particle diameter.

7.3 SEM analysis

Solutions from acid hydrolysis at 45 °C were placed in the SEM equipment without first sputtering the samples with Au/Pd to understand if it was necessary to determine the size of the particles. In Figure 7.3 a high concentration of particles can be seen; however, the ability to increase resolution and magnification required sputtering of the samples with an Au/Pd layer. This sample was scanned with an acceleration voltage (AV) of 5 kV instead of 10 kV that were used on all other samples. Even with this lower AV the beam burned through the sample at higher magnifications.
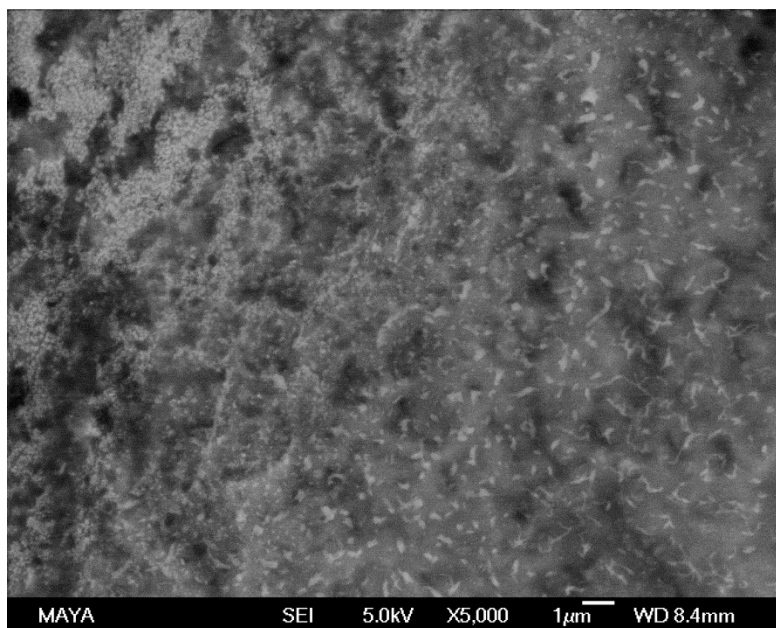

Figure 7.3. Particles can be seen at 5000 magnification without Au/Pd layer. This image shows a solution with an acid hydrolysis time of 3 hours at 45°C

The same density of particles could be found in other solutions as well. To determine if any change had occurred in the material, a sample where no acid hydrolysis had been performed was placed in the microscope after it was sputtered with Au/Pd layer. In Figure 7.4 the morphology of untreated material, a fibril structure with μm dimensions, can be viewed. When diluted more isolated particles could be found (in Figure 7.5 a fibril that is approximately 1-1,5 μm wide is displayed). Also smaller fibrils with different sizes and shapes can be seen. In addition, aggregation can be viewed around and on the larger fibril.
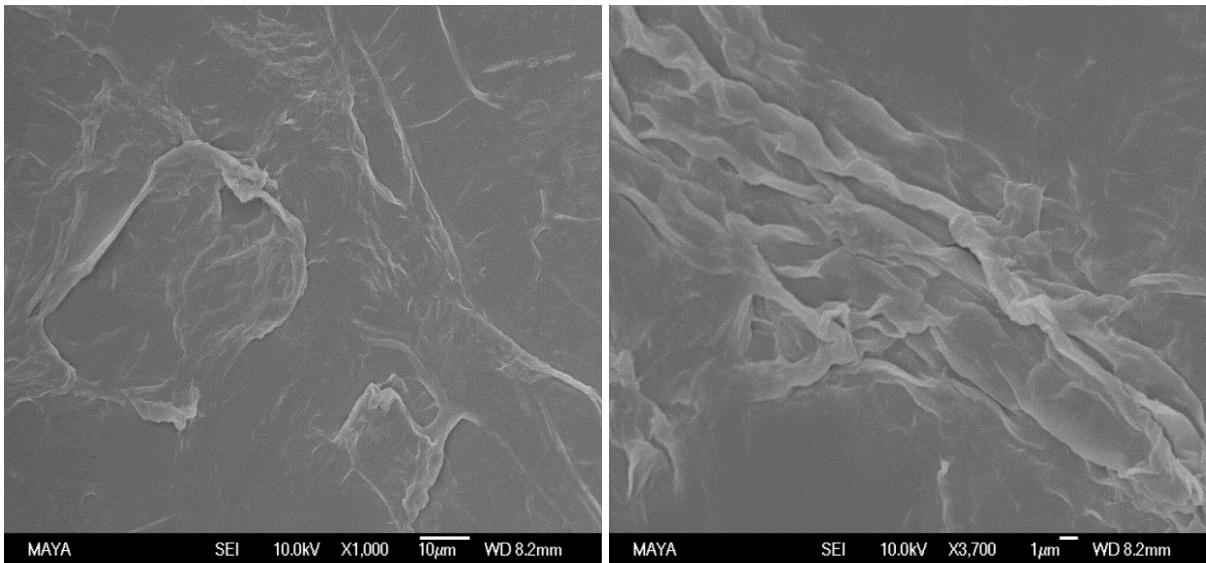
Figure 7.4. (left) Image of an untreated sample at 1000 times magnification. The image shows a fibril structure(at 1000 magnification) that is tens of μm long and just a few μm wide, which can be seen at larger magnification (3700) in the image to the right
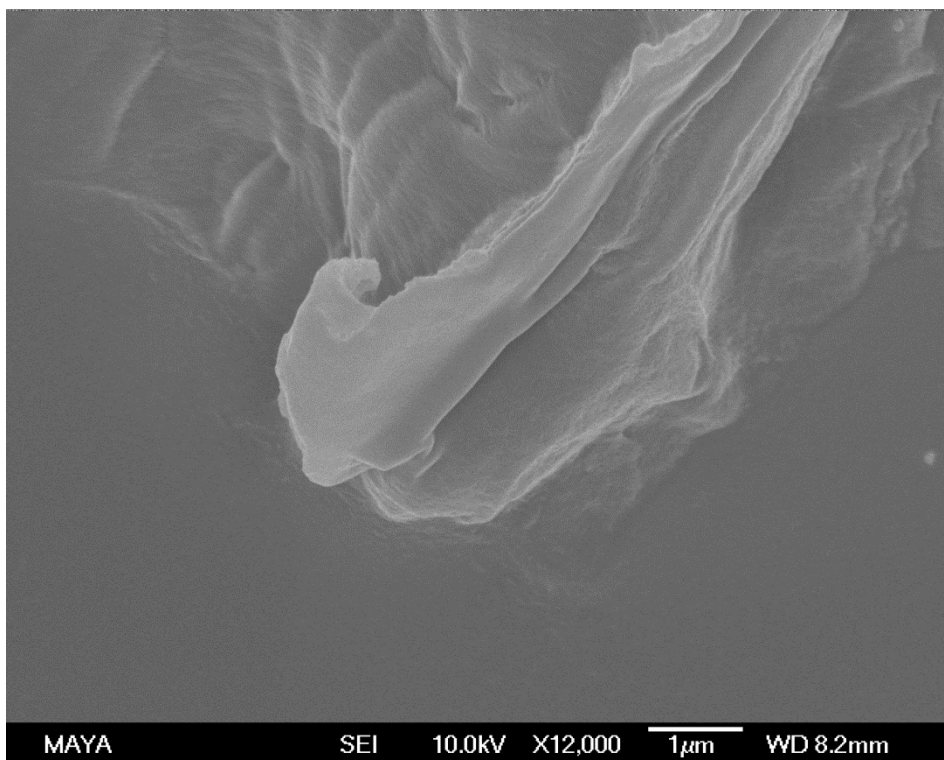

Figure 7.5. Sample from untreated material that was diluted 100 times with deionized water, at 12000 times magnification. The image shows aggregation of larger particle with smaller particles.

Figure 7.6 shows that aggregation occurs in untreated material, and that it has a fibril structure, which also Figure 7.4 suggests. In Figure 7.6 fibrils are entangled and form aggregates which are not easily broken.
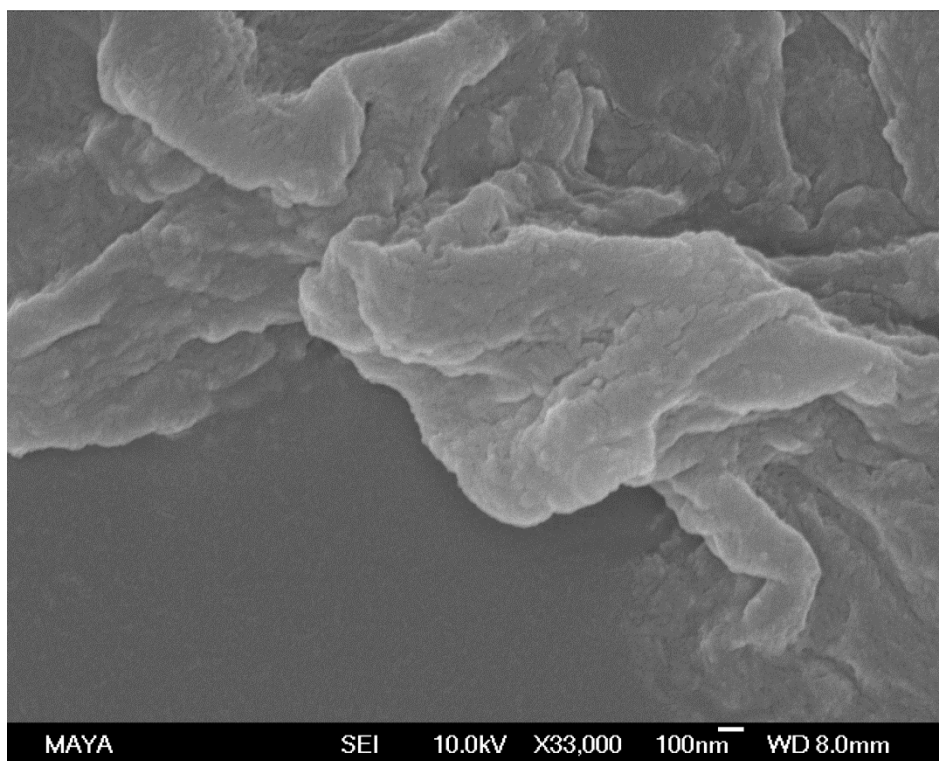
Figure 7.6. Sample from untreated material that was diluted 10 times with deionized water, at 33000 times magnification. Aggregation of smaller fibrils with lengths of 100s of nm.

A comparison of the produced nanocellulose to a commercial product supplied from Borregaard A/S was made. This product shows an entangled network of fibrils that can be viewed in Figure 7.7. Nanocellulose sample supplied from Borregaard The fibrils are μm long while nm wide, so they can be regarded as CNF. A more magnified image of the same sample can be viewed in Figure 7.8. It aggregates to the same degree as the other samples dissolved in water, which also can be seen in the figures.
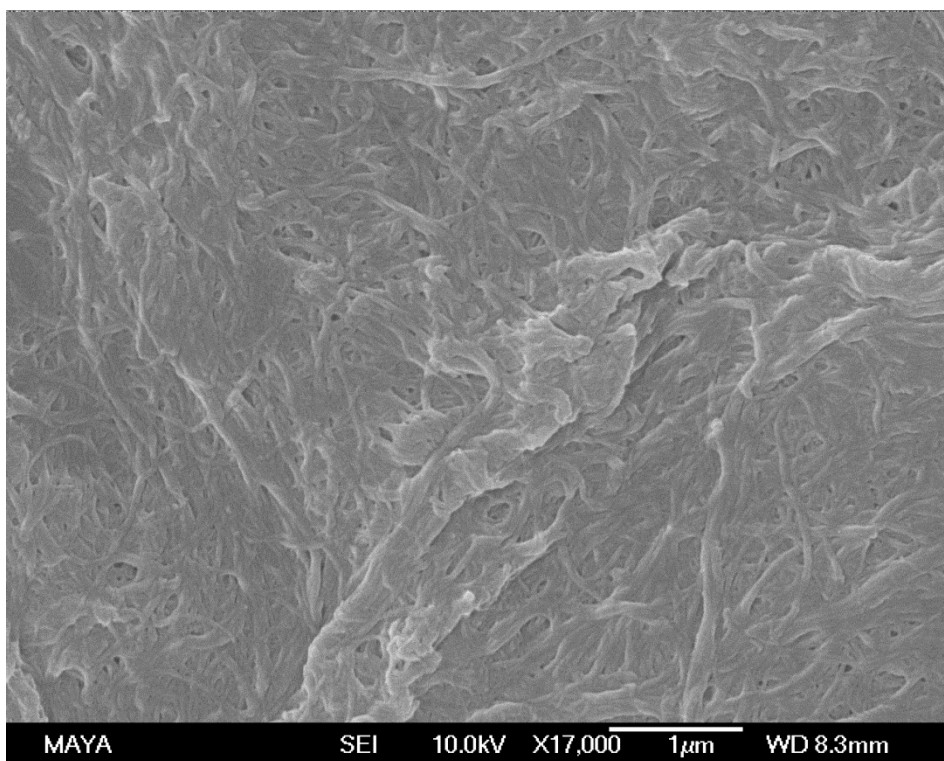
Figure 7.7. Nanocellulose sample supplied from Borregaard A/S with a magnification of 17000 (diluted 100 times)
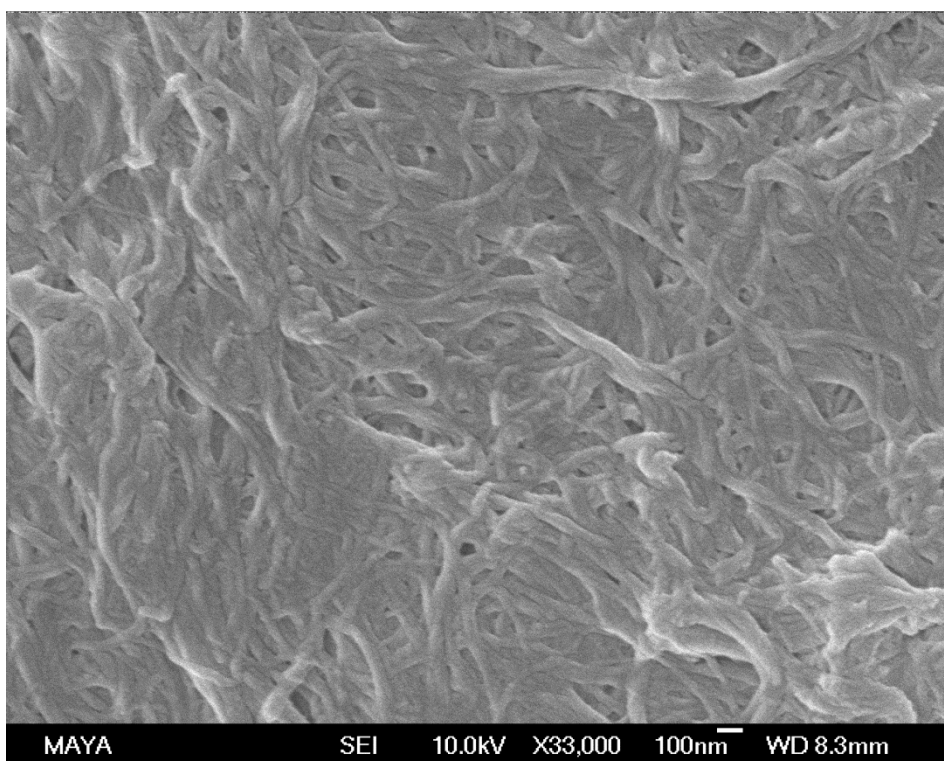

Figure 7.8. Nanocellulose sample supplied from Borregaard A/S with a magnification of 33000 (diluted 100 times)

Material treated by acid hydrolysis at 45 °C for 5 hours can be viewed in Figure 7.9. Still aggregation occurs, but smaller particles can be resolved compared to the particles in Figure 7.5, which indicates that some shortening of the chains have occurred during acid hydrolysis. Figure 7.9 shows material treated for 5 hours, which resembles a powder. A layer of Au/Pd approximately 15 nm thick coated, which the sample, indicates that the smaller particles are very small. That is, they consisted of only a small amount of chains in each polymer. Therefore, an acid hydrolysis time of 5 hours seems to be too long as the chains become very short. These figures can confirm that aggregation occurs both in untreated and treated material when suspended in water. This explains why DLS analysis will overestimate particle dimensions, because it cannot differentiate between aggregates and single particles.
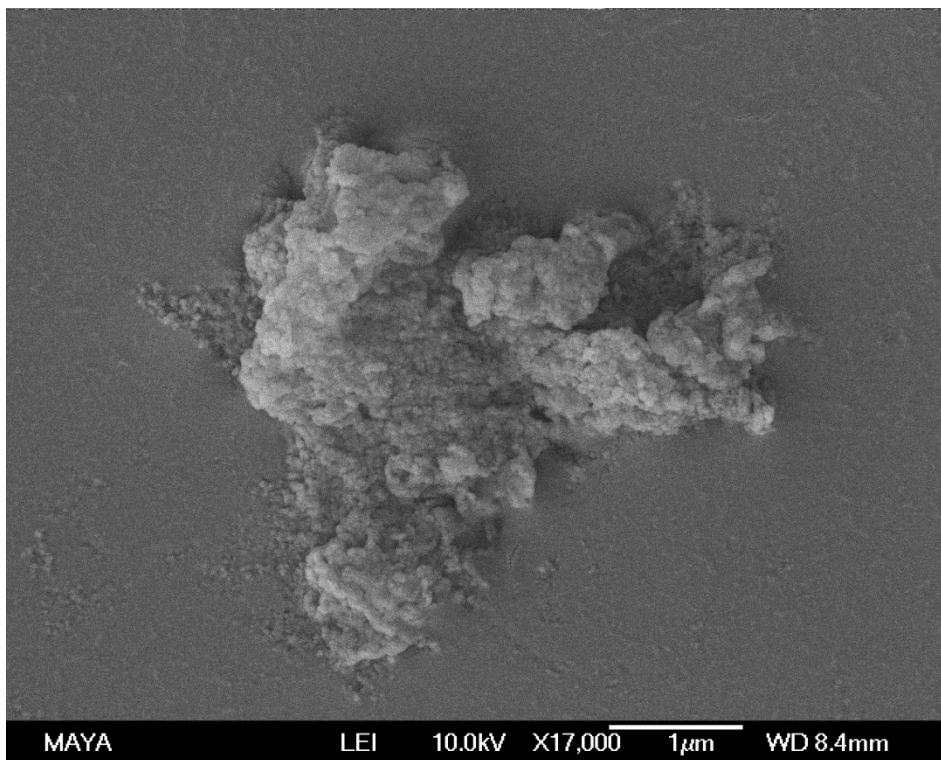

Figure 7.9. Treated material by acid hydrolysis at 45 °C for 5 hours at 17000 times magnification.

Figure 7.10 shows a sample that has much smaller dimensions than untreated material in Figure 7.5 but the fibril structure is intact. Aggregation occurs which makes it hard to isolate a single fibril and measure it. Nevertheless, fibrils that are 70 nm wide and 800 nm long can be seen.
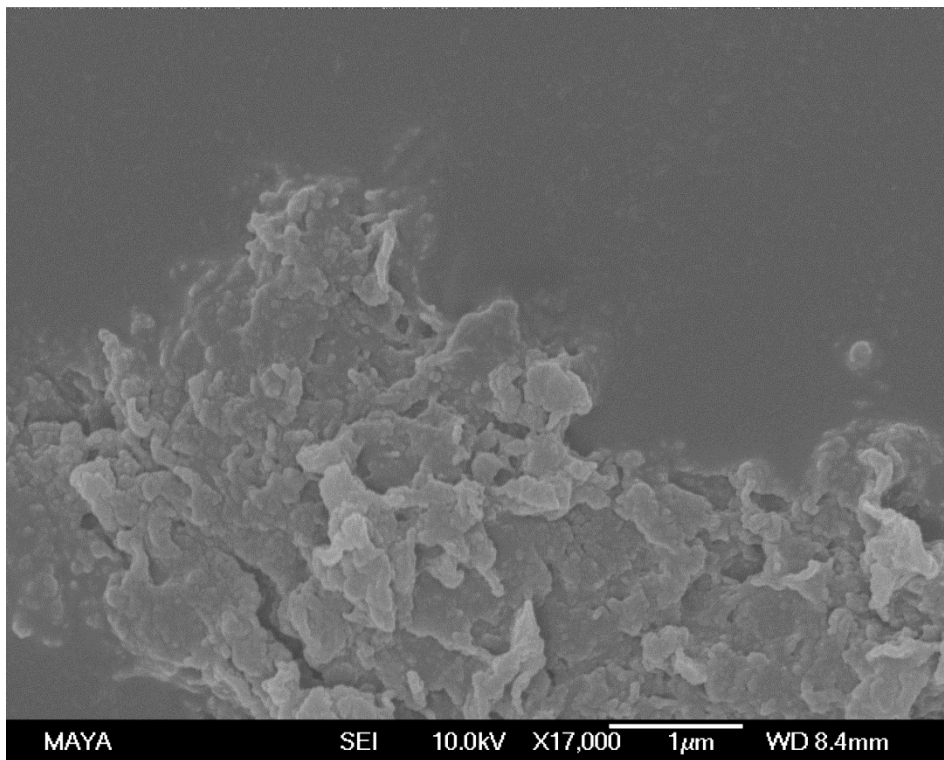

Figure 7.10. Images of sample that has been acid hydrolysed for 3 hours in 50 °C and diluted 10 times at 17000 times magnification.

The same material that was treated by acid hydrolysis for 3 hours at 50 °C can be viewed in Figure 7.11. This structure seems to be circular including many particles that also have aggregated. A single spherical particle has a diameter around 80-100 nm, which is much lower than the 226 ±1.4 nm suggested by the DLS analysis of the same sample. Compared to the structure shown in Figure 7.6 the fibril structure is removed and a smaller and circular structure has been formed instead after acid hydrolysis. This sample contains both spherical particles and fibril ones, but spherical particles are more representative of the sample as they were more common.
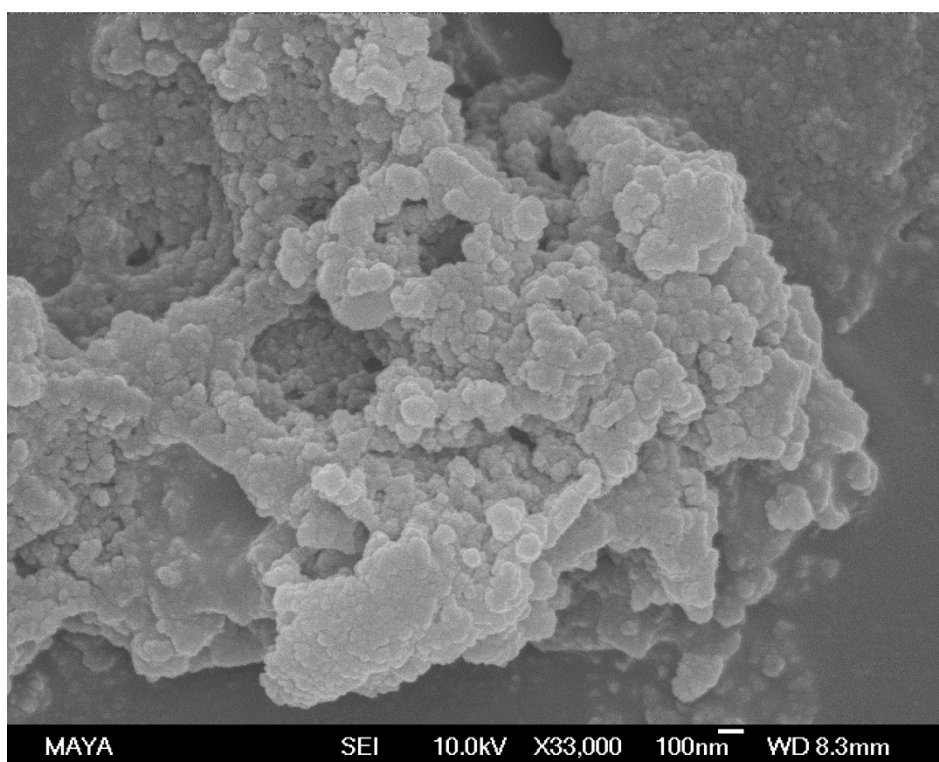

Figure 7.11. Treated material by acid hydrolysis at 50 °C for 3 hours and diluted 100 times at 33000 times magnification.

A closer look on the circular particles in Figure 7.11 reveals that one circular particle may be composed of smaller particles that have aggregated to form the larger aggregates. One of these smaller circular particles could be as small as ~20 nm in diameter; an example can be viewed in Figure 7.12. Another possibility is that one circular particle is a single particle with an uneven surface that appears to be many small particles. It can also be small rods that have aggregated and formed this spheres as literature suggests could happen [26].
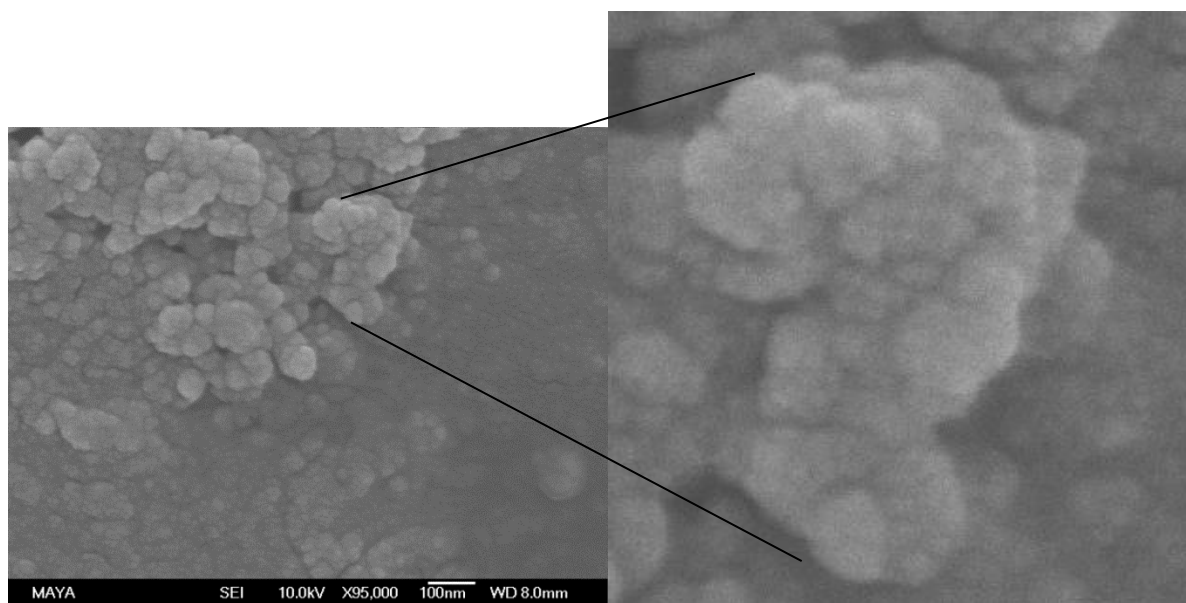

Figure 7.12. Treated material by acid hydrolysis at 50 °C for 3 hours and diluted 100 times at 95000 times magnification.. A digital magnification of that specific area can be seen to the right to illustrate the smaller particles that make up the spheres.

7.4 XRD analysis

All analysis was performed using reflection mode, which means that only data from the surface is measured. This means that the surface needs to be representative for the whole material to give an accurate estimation of the entire sample's crystallinity. With nanoparticles the surface will be a large part of the total mass, which differ from materials with bigger dimensions where the bulk represents most of the mass. This validates the assumption that the surface represents the whole material; therefore, XRD using reflection mode could be used to determine crystallinity instead of transmission where the beam goes through the sample. XRD was preformed to evaluate the crystallinity of the samples. First, the crystallinity was determined in the untreated material: The XRD pattern can be viewed in Figure 7.13. Peaks can be seen around 22 and 16 degrees, which correspond with the peaks mentioned for *cellulose I* in chapter 4. Therefore, the crystallinity of the untreated material can be calculated according to the equation in chapter 4, which results in a crystallinity of 32%.
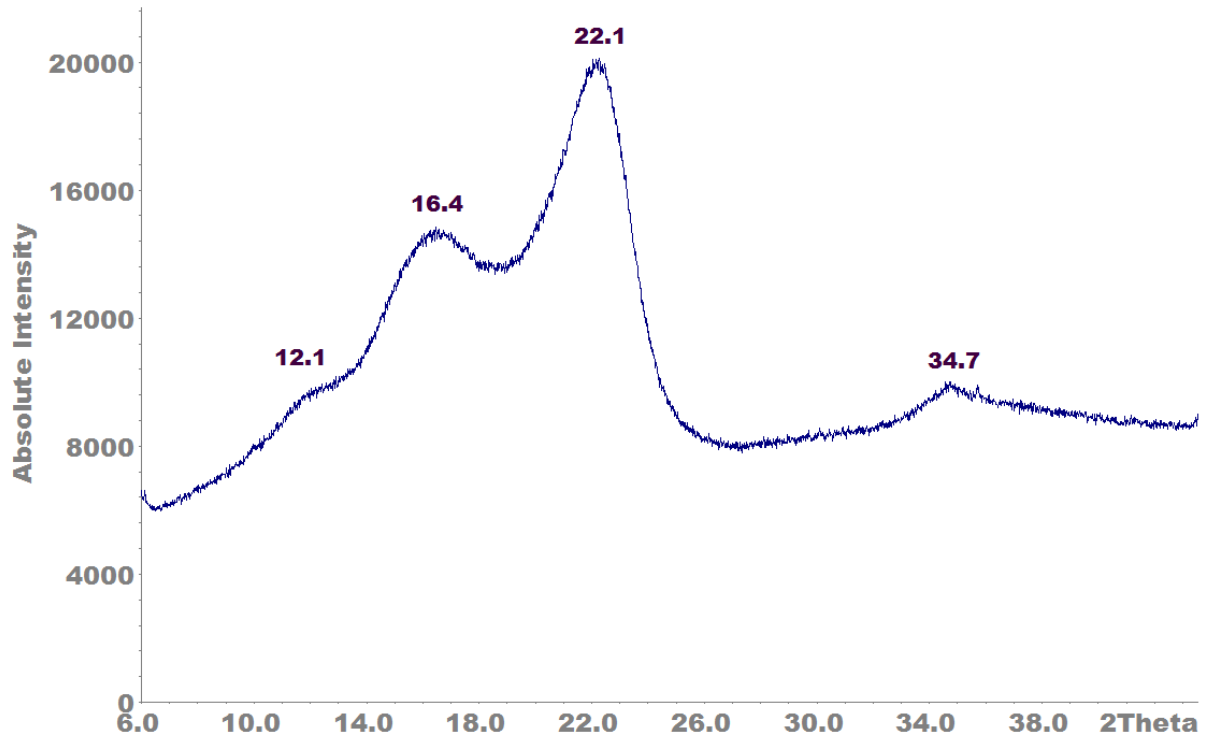
Figure 7.13. XRD pattern using reflection mode of untreated material. The x-axis shows the 2θ angle where the peaks corresponding angle can be seen in the image above the peak, each peak represents a plane in the structure. The y-axis shows the intensity of the signal detected, higher intensity means more signal.

To compare with a commercial product XRD was done on nanocellulose from Borregaard A/S, see Figure 7.14, and its crystallinity can be calculated to 36%, which is in the same range as that of the untreated material from Xylophane AB.
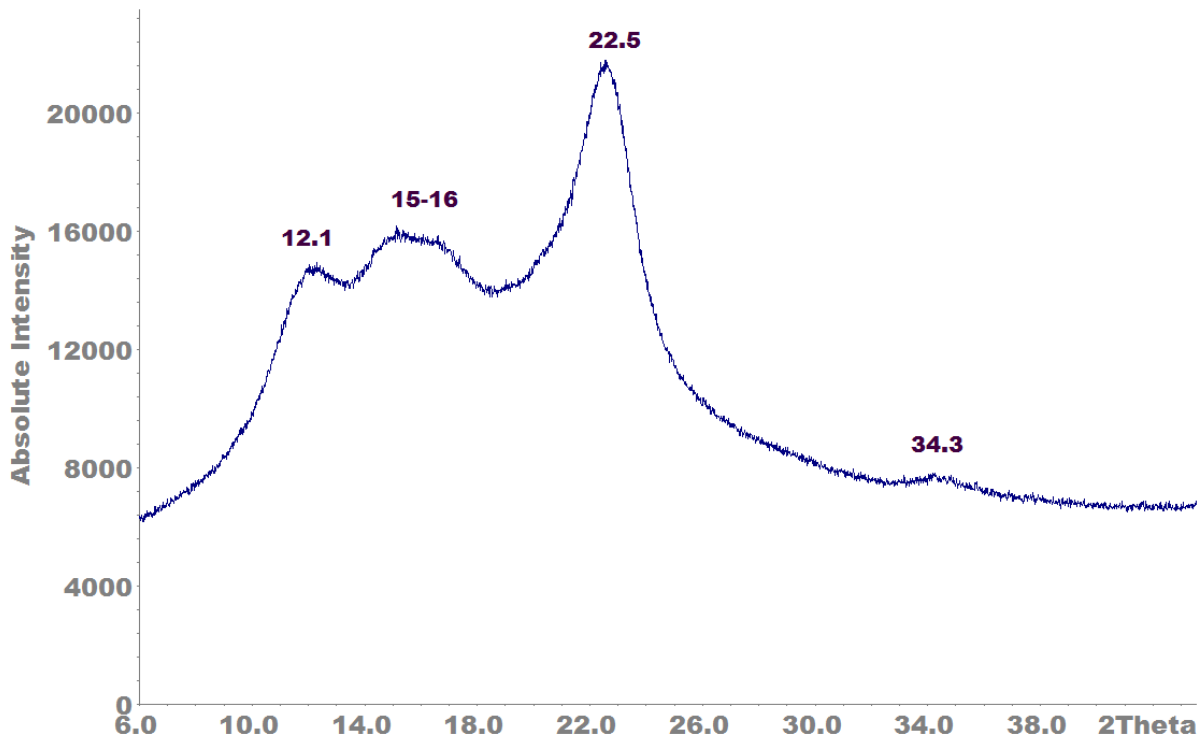

Figure 7.14. XRD pattern using reflection mode of nanocellulose from Borregaard A/S. The x-axis shows the 2θ angle where the peaks corresponding angle can be seen in the image above each peak, a peak represents a plane in the structure. The y-axis shows the intensity of the signal detected, higher intensity means more signal.

Figure 7.15 shows both the nanocellulose sample and the untreated material in the same image. As can be seen they have much in common. They both have peaks at around 16°, 22° and 34° which all correspond to *cellulose I*. The major difference is the peak around 12° that corresponds to *cellulose II*. It exists in both samples but in the sample from Borregaard A/S this peak is much more well-defined than in the untreated sample. This shows us that the Borregaard A/S sample is most likely a mixture of *cellulose I* and *cellulose II* to a greater extent than the untreated material, which is more likely to mainly consist of *cellulose I*. However, this is not considered when calculating the crystallinity, which means that the method used will yield a lower crystallinity value.
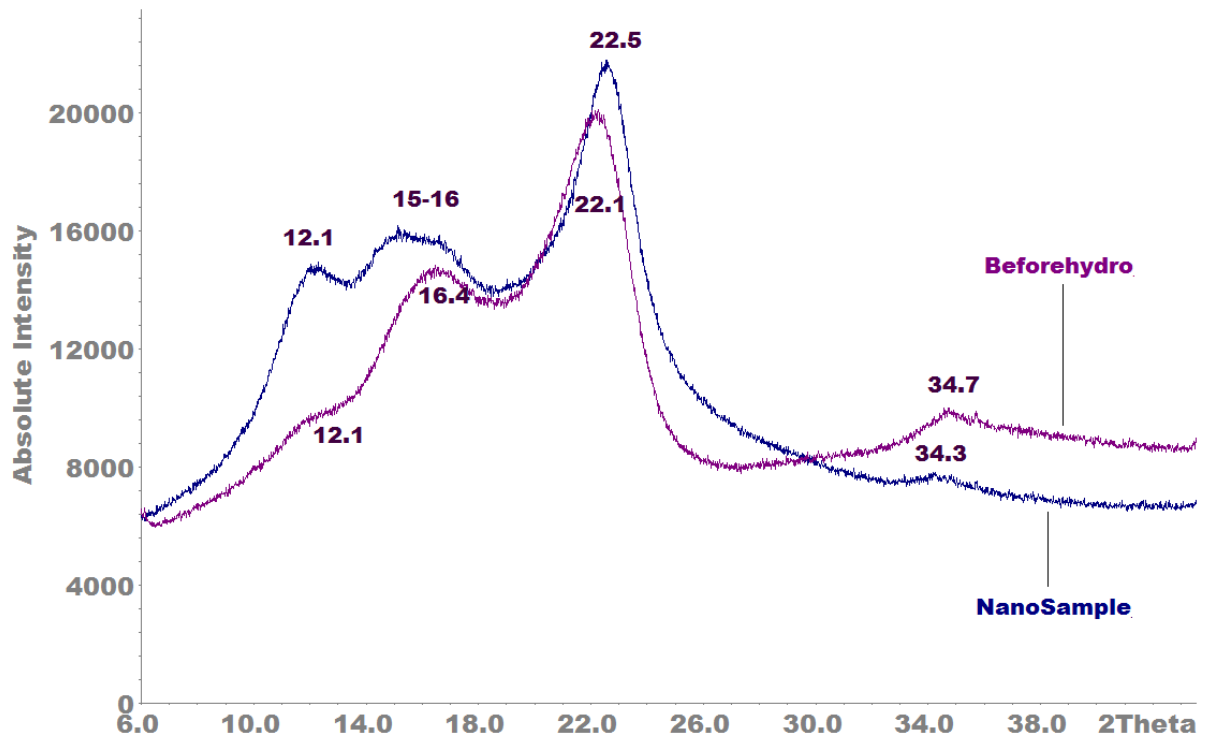

Figure 7.15. XRD patterns using reflection mode of before treatment (blue) and a nanocellulose sample from Borregaard A/S (purple) The x-axis shows the 2θ angle where the peaks corresponding angle can be seen in the image above each peak, a peak represents a plane in the structure. The y-axis shows the intensity of the signal detected, higher intensity means more signal.

The XRD pattern of a treated material can be seen in Figure 7.16. All the treated samples shown have the same peaks: one at 12° corresponding to *cellulose II* and one at 22° corresponding to *cellulose I*. Material treated for 1h, however, also have a peak around 20° which also corresponds to *cellulose II*. The peak around 34° cannot be clearly distinguished and it is assumed to be hidden in the background noise. This means that the acid hydrolysis sample contains both *cellulose I* and *II*, which is the same as the untreated material.
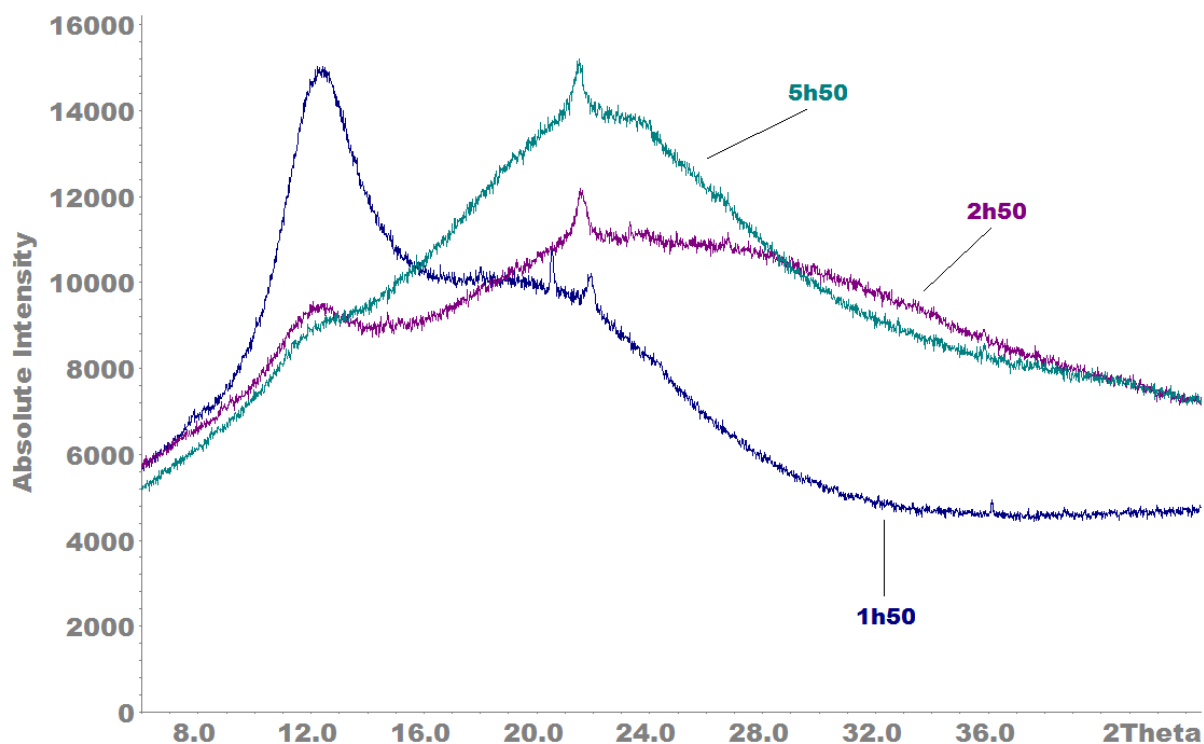

Figure 7.16. Pattern overview of XRD pattern using reflection mode of treated samples (blue 1h acid hydrolysis, purple 2h, teal 5h). The x-axis shows the 2θ angle, a peak represents a plane in the structure. The y-axis shows the intensity of the signal detected, higher intensity means more signal.

Figure 7.17 shows the treated material together with untreated to give an overview of the changes in the material structure. The untreated material consists of both *cellulose I* and *cellulose II* but favouring *cellulose I*. After one hour of acid hydrolysis this changes, the material changes to favouring *cellulose II*, as the peaks around 14-16° disappears while the peak around 12° becomes higher. The peak around 20° can be distinguished in the one-hour sample; however, this does not mean that it is not present in the untreated material, since an overlap of the larger peak around 22° and included in that peak. Under these hydrolysis conditions *cellulose I* is likely easier degraded, as the intensity becomes less for peaks associated with *cellulose I* while the *cellulose II* peaks remains more or less unchanged. This implies that the ratio of *cellulose I/cellulose II* has shifted after acid hydrolysed treatment to make *cellulose II* the most common structure. Material that has been hydrolysed for 2 h shows an intensity for the peak around 12° that has become considerable smaller. It has also become

broader, which indicates that more crystalline regions have been destroyed. The peak around 20° has disappeared, while a small peak around 22° still is present in the sample. As the hydrolysis time increases, more and more crystalline regions are destroyed so a decrease in peak intensity would be expected. This pattern can be seen in Figure 7.17 where the peak around 12° decreases with hydrolysis time. After 5 hours there is for the most part only a peak around 22° left. This could indicate that *cellulose I* is more resistant to long exposure of acid hydrolysis. However, this is an indication that the crystallinity from untreated material is preserved through the acid hydrolysis and crystalline particles are present in the samples.
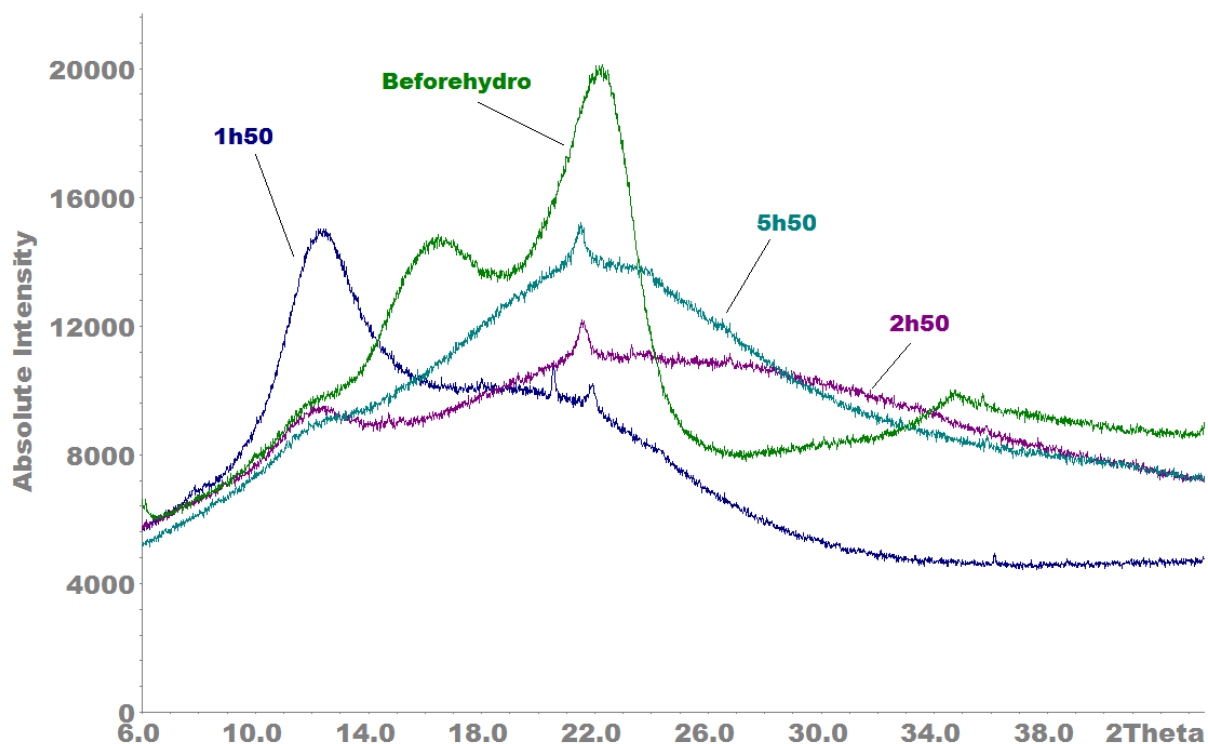
Figure 7.17. Overview of XRD pattern using reflection mode of treated samples and untreated sample (blue 1h acid hydrolysis, purple 2h, teal 5h, green untreated). The x-axis shows the 2θ angle, a peak represents a plane in the structure. The y-axis shows the intensity of the signal detected, higher intensity means more signal.

On possible explanation that the same peaks in the different samples could alternate in a small interval, is that when the XRD instrument is changed from transmission mode to reflection mode it has to be recalibrated. This could possibly add a small deviation between samples and explain why not the same plan has precisely the same 2θ angle in for example Figure 7.17.

8 Conclusion

This study was performed to investigate if it is possible to convert cellulose from alkali-extracted wheat bran to nanocellulose. By using a well-documented procedure for production of nanocellulose, i.e. by employing acid hydrolysis using sulphuric acid, nanocellulose with a mixed content of crystalline *cellulose I* and *cellulose II* could be synthesised, favouring *cellulose II*. The DLS studies yielded larger particles in the nm to μm scale, which indicated aggregation of particles. SEM studies supported the evidence of aggregation and revealed that the aggregates were made up of clusters of spheres with nano-dimensions ranging from a diameter of 80 to100 nm.

9 Future work

The acid hydrolysis needs to be optimised for alkali-extracted wheat bran, so that a better yield is achieved. The effect of hydrolysis time should be investigated, e.g. test even shorter times than 1 hour to see how this affects the structure. A change of acid to pulp ratio, acid concentration and temperature is also of importance to understand the effects on structural changes. Different acids could also be interesting to try with its own optimisation of temperature, acid concentration, acid hydrolysis time and acid to pulp ratio. Interesting analysis methods to add is Fourier transform infrared spectroscopy (FTIR), to measure the crystallinity and compare with the XRD results. For the XRD different drying techniques for the sample preparations is recommended, as drying the material affects how it looks and behaves which can give inaccurate results. The literature distinguishes between dried nanocellulose and never dried nanocellulose as the properties change upon drying. The structure should also be examined by TEM and SEM when different drying methods have been used to give better understanding of its morphology and how this changes when dried. It will also be of interest to produce larger quantities to be able to test the rheology of a solution with different concentrations of nanocellulosa, as nanocellulosa often is used as a thickener.

References

[1] L. Stevenson, F. Phillips, K. O'sullivan and J. Walton, "Wheat bran: its composition and benefits to health, a European perspective," *International Journal of Food Sciences and Nutrition,* 63: 1001-1013, 2012.

[2] M. Prückler, S. Siebenhandl-Ehn, S. Apprich, S. Höltinger, C. Haas, E. Schmid and W. Kneifel, "Wheat bran-based biorefinery 1: Composition of wheat bran and strategies of functionalization," *LWT - Food Science and Technology,* 56(2): 211-221, 2014.

[3] A. Höije, M. Gröndahl, K. Tommeraas and P. Gatenholm, "Isolation and characterization of physicochemical and material properties," *Carbohydrate Polymers,* 61: 266-267, 2005.

[4] G.-G. Chen, X.-M. Qi, Y. Guan, F. Peng, C.-L. Yao and R.-C. Sun, "High Strength Hemicellulose-Based Nanocomposite Film for Food," *ACS Sustainable Chemistry & Engineering,* 4(4): 1985-1993, 2016.

[5] A. D. Ning Lin, "Nanocellulose in biomedicine: Current status and future," *European Polymer Journal,* 59: 302-306, 2014.

[6] S. Kalia, B. S. Kaith and I. Kaur, Cellulose Fibers: Bio- and Nano-Polymer Composites, Heidelberg: Springer, 2011, 12, 45.

[7] A. C. f. life, "The Anselme Payen Award," ACS Chemistry for life, 26 March 2016. [Online]. Available: http://cell.sites.acs.org/anselmepayenaward.htm. [Accessed 24 January 2017].

[8] S. Ummartyotin and H. Manuspiya, "A critical review on cellulose: From fundamental to an approach on sensor technology," *Renewable and Sustainable Energy Reviews,* 41: 403-404, 2014.

[9] Y. Xu, Y. Dzenis and M. Hanna, "Water solubility, thermal characteristics and biodegradability of extruded starch acetate foams," *Industrial crops and products,* 21(3): 361-362, 2004.

[10] T. Larsson, "Cellulose for textiles," Innventia, [Online]. Available: http://www.innventia.com/en/Our-Expertise/Chemical-Pulping-and-bleaching/Biorefinery-products/Specialty-cellulose-for-textiles/. [Accessed 07 November 2016].

[11] D. Kim, "Nitrocellulose," *Reference Module in Biomedical Sciences,* 3: 540, 2014.

[12] D. Klemm, B. Heublein, H.-P. Fink and A. Bohn, "Cellulose: Fascinating Biopolymer

and Sustainable Raw Material," *Angewandte Chemie,* 44: 3358-3365, 2005.

[13] P. Ulvskov and H. V. Scheller, "Hemicelluloses," *Annual Review of Plant Biology,* 61: 263-281, 2010.

[14] M. Aguedo, C. Vanderghem, D. Goffin, A. Richel and M. Paquot, "Fast and high yield recovery of arabinose from destarched wheat bran," *Industrial Crops And Products,* 43: 318-320, 2013.

[15] V. H. Pomin, "Phylogeny, structure, function, biosynthesis and evolution of sulfated galactose-containing glycans," *International Journal of Biological Macromolecules,* 84: 373, 2016.

[16] L. yu, W. Zhang, T. Zhang, B. Jiang and W. Mu, "Efficient biotransformation of D-fructose to D-mannose by a thermostable D-lyxose isomerase from Thermosediminibacter oceani," *Process Biochemistry,* 51(12): 2026, 2016.

[17] F. Lionetto, R. D. Sole, D. Cannoletta, G. Vasapollo and A. Maffezzoli, "Monitoring Wood Degradation during Weathering by Cellulose Crystallinity," *Advances in Cellulosic Materials,* 5: 1910-1912, 2012.

[18] A. Naseem, S. Tabasum, K. M. Zia, M. Zuber, M. Ali and A. Noreen, "Lignin-derivatives based polymers, blends and composites: A review," *International Journal of Biological Marcomolecules,* 93: 298, 2016.

[19] W. Mulder, R. Gosselink, M. Vingerhoeds, P. Harmsen and D. Eastham, "Lignin based controlled release coatings," *Industrial Crops and Products,* 34(1): 915-916, 2001.

[20] M. Norgren and H. Edlund, "Lignin: Recent advances and emerging applications," *Current Opinion in Colloid & Interface Science* 19: 409-413, 2014.

[21] T. Abitbol, A. Rivkin, Y. Cao, Y. Nevo, E. Abraham, T. Ben-Shalom, S. Lapidot and O. Shoseyov, "Nanocellulose, a tiny fiber with huge applications," *Current Opinion in Biotechnology,* 39: 76-82, 2016.

[22] M. L. Corral, P. Cerrutti, A. Vazquez and A. Califano, "Bacterial nanocellulose as a potential additive for wheat bread," *Food Hydrocolloids,* 67: 189-190, 2017.

[23] M. Azeredoa, M. F. Rosaa and L. H. C. Mattoso, "Nanocellulose in bio-based food packaging applications," *Industrial Crops and Products,* 97: 664-665, 668, 2016.

[24] J. Zhanga, T. J. Elderb, Y. Puc and A. J. Ragauskas, "Facile synthesis of spherical cellulose nanoparticles," *Carbohydrate Polymers,* 69: 608-610, 2007.

[25] X.-f. Li, E.-y. Ding and G.-k. LI, "A method of preparing spherical nano-crystal cellulose with mixed crystalline forms of cellulose I and II," *Chinese Journal of Polymer Science,* 19(3): 291-296, 2001.

[26] P. Lu and Y.-L. Hsieh, "Preparation and properties of cellulose nanocrystals: Rods, spheres, and network," *Carbohydrate Polymers,* 82: 331-333, 2010.

[27] L. Brinchia, F. Cotanaa, E. Fortunatib and J. Kenny, "Production of nanocrystalline cellulose from lignocellulosic biomass: Technology and applications," *Carbohydrate Polymers,* 94: 157-161, 2013.

[28] R. J. Moon, A. Martini, J. Nairn, J. Simonsen and J. Youngblood, "Cellulose nanomaterials review: structure, properties and nanocomposites," *The Royal Society of Chemistry 2011,* 40: 3947-3950, 2011.

[29] H. V. Lee, S. B. A. Hamid and S. K. Zain, "Conversion of Lignocellulosic Biomass to Nanocellulose: Structure and Chemical Process," *The Scientific World Journal,* 2014: 10-12, 2014.

[30] A. Mandal and D. Chakrabarty, "Isolation of nanocellulose from waste sugarcane bagasse (SCB) and its characterization," *Carbohydrate Polymers,* 86: 1292, 2011.

[31] J. P. S. Moraisa, M. d. F. Rosab, M. d. s. M. d. S. Filhob, L. D. Nascimentoa, D. M. d. Nascimentob and A. R. Cassalesb, "Extraction and characterization of nanocellulose structures from raw cotton linter," *Carbohydrate Polymers,* 91: 230, 2013.

[32] X. M. Dong, J.-F. Revol and D. G. Gray, "Effect of microcrystallite preparation conditions on the formation of colloid crystals of cellulose," *Cellulose,* 5(1): 19-31, 1998.

[33] T. Kos, A. Anžlovar, M. Kunaver, M. Huskić and E. Žagar, "Fast preparation of nanocrystalline cellulose by microwave-assisted hydrolysis," *Cellulose,* 21(4): 2580-2584, 2014.

[34] C. Ciron, V. Gee, A. Kelly and M. Auty, "Comparison of the effects of high-pressure microfluidization and conventional homogenization of milk on particle size, water retention and texture of non-fat and low-fat yoghurts," *International Dairy Journal,* 20: 314, 2010.

[35] P. A. Penttilä, A. Várnai, J. Pere, T. Tammelin, L. Salmén, M. Siika-aho, L. Viikari and R. Serimaa, "Xylan as limiting factor in enzymatic hydrolysis of nanocellulose," *Bioresource Technology,* 129: 135-136, 2013.

[36] Z. Karim, S. Afrin, Q. Husain and R. Danish, "Necessity of enzymatic hydrolysis for production and functionalization of nanocelluloses," *Critical Reviews in Biotechnology,* 37(3): 360-362, 2017.

[37] R. Wachala, T. Ramiega, A. Kaczmarek and T. Antczak, "Nanocellulose by enzymatic methods," Annual International Conference on Composites or Nano Engineering, Canary Islands, Spain, July 21-27, 2013.

[38] C. Fritz, B. Jeuck, C. Salas, R. Gonzalez, H. Jameel and O. J. Rojas, "Nanocellulose and Proteins: Exploiting Their Interactions for Production, Immobilization, and Synthesis of Biocompatible Materials," *Advances in Polymer Science,* 271: 208-211, 2015.

[39] T. Saito, M. Hirota, N. Tamura, S. Kimura, H. Fukuzumi, L. Heux and A. Isogai, "Individualization of Nano-Sized Plant Cellulose Fibrils by Direct Surface Carboxylation Using TEMPO Catalyst under Neutral Conditions," *Biomacromolecules,* 10: 1992–1996, 2009.

[40] A. Isogai and T. Saito, "TEMPO-Mediated Oxidation of Native Cellulose. The Effect of Oxidation Conditions on Chemical and Crystal Structures of the Water-Insoluble Fractions," *Biomacromolecules,* 5: 1983-1984,1987-1988, 2004.

[41] T. Saito, S. Kimura, Y. Nishiyama and A. Isogai, "Cellulose Nanofibers Prepared by TEMPO-Mediated Oxidation of Native Cellulose," *Biomacromolecules,* 8: 2487-2490, 2007.

[42] E. N. J. Ford, S. K. Mendon, S. F. Thames and J. W. Rawlins, "X-ray Diffraction of Cotton Treated with Neutralized Vegetable Oil-based Macromolecular Crosslinkers," *Journal of Engineered Fibers and Fabrics,* 5(1): 14, 2010.

[43] S. Park, J. O. Baker, M. E. Himmel, P. A. Parilla and D. K. Johnson, "Cellulose crystallinity index: measurement techniques and their impact on interpreting cellulase performance," *Biotechnology for Biofuels,* 3(10): 2-4, 2010.

[44] N. Terinte, R. Ibbett and K. C. Schuster, "Overview on native cellulose and microcrystalline cellulose I structure studied by X-ray diffraction (WAXD): Comparison between measurement techniques," *Lenzinger Berichte,* 89: 121-122, 2011.

[45] A. Sluiter, B. Hames, R. Ruiz, C. Scarlata, J. Sluiter, D. Templeton and D. Crocker, "Determination of Structural Carbohydrates and Lignin in Biomass, Laboratory Analytical Procedure-002, 003, 017, 019," National Renewable Energy Laboratory, U.S. Department of Energy, USA, 2008.

[46] F. Carvalheiro, L. C. Duarte and F. M. Gírio, "Hemicellulose biorefineries: a review on biomass pretreatments," *Journal of Scientific & Industrial Research,* 67: 852-858, 2008.

[47] S. I. Njoku, J. A. Iversen, H. Uellendahl and B. K. Ahring, "Production of ethanol from hemicellulose of cocksfoot grass using pichia stipitis," *Sustainable Chemical Processes,* 1: 1-2, 2013.